Łukasiewicz
Łódzki Instytut Technologiczny

TECHNOLOGIA I JAKOŚĆ WYROBÓW

Czasopismo Naukowe
Sieci Badawczej Łukasiewicz – Łódzkiego Instytutu Technologicznego

Rocznik 69/2024
ISSN-2299-7989

TECHNOLOGIA I JAKOŚĆ WYROBÓW ROCZNIK ŁUKASIEWICZ – ŁÓDZKIEGO INSTYTUTU TECHNOLOGICZNEGO
ISSN 2299-7989

Wydawca
Sieć Badawcza Łukasiewicz –
Łódzki Instytut Technologiczny
91 - 463 Łódź, ul. Zgierska 73

Przedmowa

Szanowni Czytelnicy,

zachęcam do lektury artykułów naukowych ujętych w najnowszym wydaniu rocznika.

Czasopismo wydawane jest w trybie open access, bez opłat publikacyjnych, a językiem publikacji jest angielski. Rocznik stosuje zasady etyki publikacyjnej COPE, jest także indeksowany w bazach: ERIH Plus, Chemical Abstracts, BAZ – TECH. Artykuły posiadają identyfikację elektronicznych wersji publikacji naukowych DOI.

Systematycznie zwiększamy zakres tematyczny prac ujętych w naszym czasopiśmie. Aktualnie Redakcja realizuje szereg wielopłaszczyznowych działań mających na celu usprawnienie procesu wydawniczego, podniesienie doskonałości naukowej publikowanych prac oraz ich umiędzynarodowienie, przy jednoczesnym wzroście rozpoznawalności rocznika Technologia i Jakość Wyrobów (TJW), zwłaszcza w zagranicznych środowiskach naukowych.

Serdecznie zapraszam do dalszej współpracy i życzę kolejnych sukcesów wraz z naszą Redakcją.

Redaktor Naczelna,

dr hab. inż. Katarzyna Ławińska

Katarzyna Ławińska

Spis treści

Effectiveness of hand disinfection using commercial antibacterial wipes

Dorota Gendaszewska [1*], Katarzyna Miśkiewicz [1], Katarzyna Zacharska [1]

[1] Lukasiewicz Research Network - Lodz Institute of Technology, Lodz, Poland

Abstract

This paper investigated the effectiveness of hand disinfection with commercial biocidal wipes using RODAC contact plates. The highest level of bacterial reduction (100%) was obtained for W1 wipes - saturated with propanol, among others. A slightly lower, but also high level of reduction at an average of 95.5% was obtained for W3 wipes containing only ethyl alcohol. For the W2 wipes without added alcohol, the bacterial reduction rate averaged 54%. Similar results were obtained for fungi: the highest degree of reduction was achieved for W1 and W3 wipes (100%), the lowest for W2 (average 67.5%). Wipes with alcohol enriched with other active substances showed the strongest antimicrobial activity. No pathogenic microorganisms were found in any of the samples tested.

Keywords: disinfection, hand cleanliness, antimicrobial wipes, RODAC contact plates

1. Introduction

Disinfection is the destruction of pathogenic microorganisms and their spore forms in a defined external environment to prevent their spread. It's essential in order to prevent the transmission of diseases and infections and prevent unwanted microbial contamination. For disinfection, physical agents such as high temperature, sunlight, ultraviolet radiation or chemical agents, i.e. preparations with an active substance, are used [1]. The combination of these methods is referred to as a chemical-thermal process because an increased temperature accelerates the

[*] corresponding author e-mail: dorota.gendaszewska@lit.lukasiewicz.gov.pl
DOI: 10.57636/69.2024.1.1

reactions taking place [2,3]. The disinfection process uses several chemical compounds that significantly combat human-threatening bacteria, viruses and fungi. The group of compounds used in this process includes phenolic compounds, chlorine compounds, aldehydes, peroxy compounds, alcohols and surfactants, including quaternary ammonium compounds [3].

Phenol-type compounds are effective against bacteria, fungi and viruses, but have no effect on spore forms. Furthermore, they are unsuitable for disinfecting skin, medical equipment or food-related surfaces due to their toxicity and low biodegradability. Chlorine compounds are also effective against many pathogens but can corrode materials such as plastics and metal. Peroxide compounds have a similar effect; they show antibacterial and antifungal activity but can accelerate corrosion of metallic surface components. Aldehydes are employed for disinfection and sterilisation due to their comprehensive action spectrum, although they are also toxic and can cause irritant reactions. The most utilised substances for disinfection are alcohol (e.g. ethanol, isopropanol). These compounds are effective, although their efficacy is reduced when diluted with water. Quaternary ammonium compounds, also known as QACs, are effective against bacteria, fungi, and viruses but have no effect on spores [3].

Sterilization and disinfection of microorganisms have been extensively studied in order to address the problem of environmental contamination, which is a crucial issue for public health and economics [4]. For disinfectants three basic mechanisms of action are known, which depend on the chemical structure of the active substance. The first mechanism of action of disinfectants may involve damage to the cytoplasmic membranes of microorganisms by altering protein-lipid structures or by lowering surface tension, or by protein denaturation. Alcohol, aldehydes and phenols act in this way. The second mechanism of action is through inhibition of enzyme secretion by denaturation or by blocking active centers, e.g. thiol groups. Oxidizing agents, silver and mercury compounds act in this way. Sulphonamides and 5 - nitrofuran derivatives, on the other hand, react with the nucleic acids of microorganisms, leading to their destruction [5,6]. Regardless of the mechanism of action, a good disinfectant should be disinfected effectively in a short time, have a broad spectrum of action, be well tolerated by skin, mucous membranes and wounds, and be non-sensitizing and non-toxic. It should have a long shelf life and be biodegradable. Finally, it should not have an irritating odour [7].

The aim of this study was to test three types of antimicrobial wipes for their effectiveness in disinfecting the hand surfaces of office workers. Many studies show that frequently touched surfaces at a workplace such as computer keyboard, computer mouse, door handle and mobile phone touchscreens are excellent examples of places harboring various microorganisms, possibly also harmful to human health [8,9]. By frequently touching these types of surfaces, in the absence of proper hygiene, there is a risk of transferring these microorganisms to workers' hands. Therefore, which wipes are more effective for disinfection is discussed in this article.

2. Materials and Methods

2.1. Materials

To achieve the outlined objective of the work, commercially available antibacterial wipes were purchased for both hand and surface disinfection. Table 1 provides a brief description of the physical and chemical characteristics of the products tested. RODAC plates (BioMaxima S.A., Poland) were used for all tests. These contact plates allow surface sampling of bacteria (plates with composition: TSA IRR LAB-AGAR™ + Letheen + Tween) and fungi (plates with composition: Sabouraud Dextrose with chloramphenicol IRR LAB-AGAR™ + Letheen + Tween) growing on the agar medium. In addition, RapID™ STAPH PLUS System (Argenta S.A., Poland) were used to identify bacterial colonies of *Staphylococcus* spp. grown on the plates.

Tab. 1. Physical and chemical characteristics of the wipes tested.

Code	Name	Active compounds	Type	Odour
W1	Wipes for hand and surface disinfection, including surfaces of medical devices	Propane-2-ol, d-gluconic acid, compound with N,N‘’bis-(4-chlorophenyl)-3,12 dimino 2,4,11,13-tetraazatetradecanediamidine (2:1)	contains alcohols	Cashmere
W2	Alcohol-free wipes for cleaning and rapid disinfection of surfaces	N-(3-aminopropyl)-N-dodecylpropane-1,3-diamine, Poly (oxy-1,2-ethanediol), .alpha.-[2-didecylmethylamine)ethyl]-.omega.-hydroxy-,propanoate (salt).	without alcohols	No irritating odour
W3	Alcohol wipes for cleaning and disinfecting small surfaces and medical equipment	Ethanol, propan-2-ol	contains alcohols	Tea tonic

2.2. Methods

Hand cleanliness tests were carried out on all the workers tested, both before and after hand disinfection, and the degree of reduction was determined from the results. All three products (W1, W2, W3) are readily available to consumers, but have different characteristics (Table 1). The RODAC tests were selected for testing as they are a rapid and effective method for the control of microbial contamination of workers' hands [11]. The six volunteers were asked to contaminate their hands by touching typical everyday surfaces (i.e. handrails, door handles, computer mouse and keyboard) with both hands prior to testing. Next, in the microbiology laboratory, a samples of each subject's inner part from both hand was taken with RODAC contact test with TSA (Tryptic Soy Agar) for total bacterial count and RODAC contact test with SDA (Sabouraud Dextrose Agar) for total fungal count. Each volunteer tested each type of wipe in triplicate. There were no significant differences in age distribution (38-45 years) between the three groups. After applying the wipes and waiting until the hands were completely dry, samples were taken from both hands of each subject using the same type of RODAC contact test as before. The RODAC plate samples containing SDA substrate were incubated aerobically at 25±1°C for five to seven days (test for fungi) while RODAC containing TSA substrate were incubated aerobically at 36±1°C for one to two days (test for bacteria). Total colony-forming units (CFU) were manually counted for each plate after incubation (Figure 1). In cases where the number of microbial colonies was too high to be counted, a value of 150 CFU was used [10]. All the assays were assessed in triplicate, and the results were expressed as mean ± SD values of the three sets of observations ($P < 0.05$). The mean values and standard deviation were calculated using the EXCEL program from Microsoft 365 package. Finally, the grown colonies were identified using RapID™ STAPH PLUS System (Remel, Poland). Gram staining was performed to check which morphological forms were present in the contacts studied and to which type of bacteria in terms of cell wall structure they belong, i.e. whether Gram-positive or Gram-negative microorganisms. Macroscopic and microscopic observations were also made to confirm the presence of moulds and to qualify for certain genera of fungi. No additional dermatological or other clinical data were collected.

3. Results and Discussion

Figure 1 shows a RODAC agar plate with samples collected from personnel's hands before cleaning, after five days of incubation. Additionally, a microscopic image of Gram-positive bacilli isolated from RODAC plates after two days of incubation is provided, confirming microbiological contamination of the workers' hands. Effective cleaning and disinfection can help prevent the spread of microorganisms responsible for various diseases, especially among high-risk groups [12].

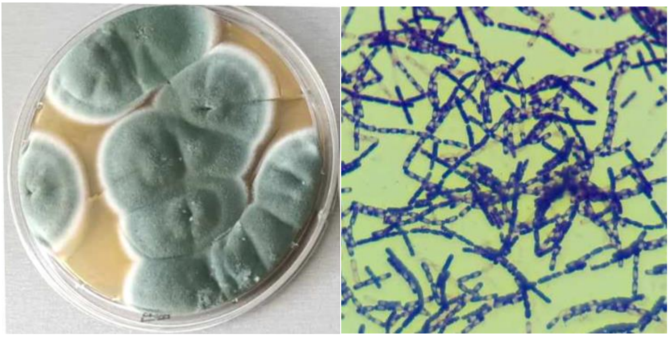

Fig. 1. Replicate Organism Detection and Counting (RODAC) agar plate, which was sampled from a hand at the middle of the workday before cleaning a) fungal culture b) microscopic image of isolated bacteria- Gram positive spore-forming bacilli, zoom 1000x (Delta Optical ProteOne, no. cat. DO-3800).

The results are shown in Table 2 and 3. When the alcohol wipes W1 and W3 were used, the level of microbial reduction was on a similar high level, ranged 100% for W1 and 95,5% for W3. However, when the alcohol-free wipes were used (W2), the bacterial reduction values were lower at 54% (Table 2).

Tab. 2. Effectiveness of disinfectant wipes in removing microorganisms (bacteria) from hands.

Code of sample	Mean % reduction ± SD (mean CFU/RODAC pre- and postcleaning) [%]					
	1	2	3	4	5	6
W1	100.0±0.0	100.0±0.0	100.0±0.0	100.0±0.0	100.0±0.0	100.0±0.0
W2	54.0±4.9	62.0±6.5	48.2±8.0	54.0±8.2	46.4±5.3	61.5±9.4
W3	96.0±3.3	90.5±3.7	100.0±0.0	96.0±4.5	94.0±4.9	96.5±2.9

± means standard deviation for n=6

It means that the greatest reduction in bacteria was observed for disinfection with wipes containing alcohol and another active substance (W1), slightly lower efficacy was observed for disinfection with wipes with alcohol alone (W3), and the lowest antimicrobial efficacy was observed for disinfection with wipes without alcohol (W2). Similar observations were made by Butz et al. (2013). They proved that repeated washing with alcohol-soaked wipes results in a reduction of bacterial colonies comparable to non-medicated soap, sufficient to prevent hand transmission of pathogens. They concluded that alcohol-soaked wipes are an acceptable alternative to washing hands with soap and water in healthcare facilities [13].

Biochemical testing of some grown isolates on RODAC plates from TSA revealed the presence of the following staphylococcal species: *Staphyloccocus auricularis* (the probability of occurrence of this species in the ERIC™ Software of numerical codes for the RapID™ STAPH PLUS System test, Remel was >99.9%), *S. cohnii ssp. cohnii* (97.05% - ERIC™ Software for RapID™ STAPH PLUS System test, Remel), *S. saprophyticus* (97.71% - ERIC™ Software for RapID™ STAPH PLUS System test, Remel) and *S. hyicus* (>99.9% - ERIC™ Software for RapID™ STAPH PLUS System test, Remel). The species very commonly lives on human skin. For example, *S. auricularis* was originally isolated from the exterior of a human ear, *S. saprophyticus* causing opportunistic infections, clinical isolates of *S. cohnii ss. cohnii* have shown high levels of antibiotic resistance. All of them may be able to cause bacteremia or sepsis [14]. Among the other types of bacteria isolated from the hands of the personnel examined, the Gram-positive spore-forming bacilli observed in many Gram-stained microscope slides should be mentioned first and foremost (Figure 1). The genus is commonly found in both natural and laboratory environments. *Bacillus* spp. develop numerous spores resistant to adverse environmental conditions, but also to many disinfectants. Infection with this type of bacteria spreads rapidly in the laboratory environment and is very difficult to eradicate [15]. No other morphological types of bacteria were observed.

Macroscopic and microscopic observations of isolated colonies from RODAC plates with SDA confirmed the presence of moulds belonging to the genera *Aspergillus* and *Penicillium*, which are the dominant group of fungal airspores worldwide. However, the concentration of fungi on the hand surface varied in the pre-cleaning group. Results for the pre-cleaning group ranged from 0 to 15 CFU/plate. No growth of fungal colonies was observed in the group after disinfection with W1 and W3 wipes, resulting in a 100% reduction of fungi (Table 3).

Tab. 3. Effectiveness of disinfectant wipes in removing microorganisms (fungi) from hands.

Code of sample	Mean % reduction ± SD (mean CFU/RODAC pre- and postcleaning) [%]					
	1	2	3	4	5	6
W1	100.0±0.0	100.0±0.0	100.0±0.0	100.0±0.0	100.0±0.0	100.0±0.0
W2	50.0±4.8	60.0±6.5	86.0±3.3	75.0±4.1	55.0±12.2	67.5±2.0
W3	100.0±0.0	100.0±0.0	100.0±0.0	100.0±0.0	100.0±0.0	100.0±0.0

For W2 the reduction was only 67.5%. This means that the alcohols in the W1 and W3 wipes, including isopropyl alcohol, are highly effective against fungi that colonise staff hands. Studies by Thaddeus et al. (2018) confirmed the efficacy of isopropyl alcohol against *C. albicans* and *A. niger*. In the concentration range of 60%-100%, isopropyl alcohol inhibited more fungal organisms than ethanol, although the diameters of the zones of inhibition it produced were not statistically different from those of ethanol [16]. The results of Nnagbo et al. (2024) showed that only one of the four alcohol-based hand sanitizers tested inhibited the growth of all tested organisms. It was both bactericidal against *E. coli, S. aureus, K. pneumoniae* and fungicidal against *C. albicans* and *A. flavus* at the highest concentration (100mg/ml) [17]. This shows how important it is to reliably inform customers about the effects of a given preparation, to effectively protect their health.

4. Conclusions

This paper investigates the effectiveness of hand disinfection using commercially available biocidal wipes. The study used RODAC contact plates, tests used for rapid diagnosis of microbial contamination. The greatest reduction in bacteria was observed for disinfection with wipes containing alcohol and another active ingredient (W1), slightly lower efficacy was observed for disinfection with wipes containing alcohol alone (W3), and the lowest antimicrobial efficacy was observed for disinfection with wipes without alcohol (W2). Similar results were observed for fungi, with W1 and W3 wipes achieving a complete reduction in fungal growth and W2 only 67.5%. The study showed that wipes with a richer composition of isopropyl alcohol and other active ingredients had an overall stronger antimicrobial effect than other wipes tested. The study described in this paper highlights the importance of hand hygiene and disinfection in preventing the spread of disease in our environment.

The research work was carried out within the project: "Łukasiewicz dla dzieci – zajęcia edukacyjne i warsztaty" financed by the National Science Centre (NdS/547246/2022/2022).

References

[1] https://encyklopedia.pwn.pl/ [accessed: 30.04.2024]
[2] Buchrieser V., Miorini T.: *Grundlagen der Reinigung, Desinfektion und Sterilisation*. WFHSS. 2009.
[3] Yemis F., Yenil N.: *Classification, Uses and Environmental Implications of Disinfectants,* Pakistan Journal of Analytical & Environmental Chemistry, [S.l.], 21 (2), 2020, pp. 179 – 192.
[4] Bharti, B., Li, H., Ren, Z., Zhu, R., & Zhu, Z.: *Recent advances in sterilization and disinfection technology: A review.* Chemosphere, 308, 2022, 136404.
[5] Bridier A., Briandet R., Thomas V., Dubois-Brissonnet F.: *Comparative biocidal activity of peracetic acid, benzalkonium chloride and ortho-phthalaldehyde on 77 bacterial strains,* Journal of Hospital Infection, 78, 2011, pp. 208-213.
[6] McDonnell G., Russell A.D.: *Antiseptics and disinfectants: activity, action, and resistance.* Clinical Microbiology Review, 12, 1999, pp. 147–179.
[7] Ziembińska A., Szpindor M.: *Comparison of the bactericidal efficacy of disinfectants on microorganisms isolated from the epidermis*, Chemik, 67 (2), 2013, pp. 127-130. [in Polish].
[8] Bures S., Fishbain J.T., Uyehara C.F., Parker J.M., Berg B.W.: *Computer keyboards and faucet handles as reservoirs of nosocomial pathogens in the intensive care unit*, Am. J. Infect. Control., 28, 2000, pp. 465–471.
[9] Brooke, J.S.; Annand, J.W.; Hammer, A.; Dembkowski, K.; Shulman, S.T.: *Investigation of bacterial pathogens on 70 frequently used environmental surfaces in a large urban U.S. university*, J. Environ. Health, 2009, 71, pp. 17–22.
[10] PN-EN ISO 7218:2008 Microbiology of food and feed - General requirements and principles of microbiological tests [in Polish]
[11] Hajar Z., Mana T.S.C., Cadnum J.L., Donskey C.J.: *Dispersal of gram-negative bacilli from contaminated sink drains to cover gowns and hands during hand washing*, Infect Control Hosp Epidemiol, 40(4), 2019, pp. 460-462.
[12] Ford B.D., Sopha C.: *An evaluation of conventional cleaning and disinfection and electrostatic disinfectant spraying in K-12 schools,* Canadian Journal of Infection Control, 35(1), 2020, pp. 35–38.

[13] Butz A. M., Laughon B. E., Gullette D. L., Larson, E. L.: *Alcohol-impregnated wipes as an alternative in hand hygiene*, American journal of infection control 18(2), 1990, pp. 70-76.
[14] Piette A., Verschraegen G.: *Role of coagulase-negative staphylococci in human disease*, Veterinary Microbiology, 134 (1–2), 2009, pp. 45-54.
[15] Sliman R., Rehm S., Shlaes D.: *Serious Infections Caused by Bacillus Species*, Medicine, 66(3), 1987, pp. 218-223.
[16] Thaddeus N. I., Francis E. C., Jane O. O., Obumneme A. C., Okechukwu, E. C.: *Effects of some common additives on the antimicrobial activities of alcohol-based hand sanitizers*, Asian Pacific Journal of Tropical Medicine, 11(3), 2018, pp. 222-226.
[17] Nnagbo P. A., Nwachukwu, I. O.: *Effectiveness Of Different Brands Of Alcohol-Based Hand Sanitizers Against Some Selected Microorganisms*, Multi-Disciplinary Research and Development Journals Int'l 5(1), 2024, pp.1-10.

Comparison of rheological properties of molasses from different sugar factories

Magdalena Orczykowska*, Andrzej Obraniak

Lodz University of Technology, Faculty of Process and Environmental Engineering, Lodz, Poland

Abstract

The paper presents a comparison of the rheological properties of raw molasses, which is a by-product in the food sugar production process, using the Ostwald de Waele power law model. For the analysis of rheological properties, molasses from a sugar factory in Bač (Serbia), a sugar factory in Elaziğ (Turkey) and a sugar factory in Glinojeck (Poland) were selected. This analysis was carried out in the temperature range from 40^{0}C to 60^{0}C.

Keywords: sugar beet, molasses, viscosity, power law model

1. Introduction

Molasses is a dark brown, thick and sweet syrup that is produced as a by-product during the production of table sugar. It contains about 20% water, 8% inorganic substances, 72% sugar and non-sugar organic substances such as organic acids, lipids and inorganic salts, invert sugar, high molecular weight macromolecules (starch, cellulose, hemicellulose, lignin, pectin, tannin) [1-3]. Depending on the raw material from which sugar is produced, beet, cane and carob molasses are distinguished [1]. Molasses is increasingly obtained from grapes [4], as well as from dates or apricots [5].

* corresponding author e-mail: magdalena.orczykowska@p.lodz.pl
DOI: 10.57636/69.2024.1.2

However, it is sugar beet, after sugar cane, that is the most important industrial plant used for sugar production in the world Fig. 1.

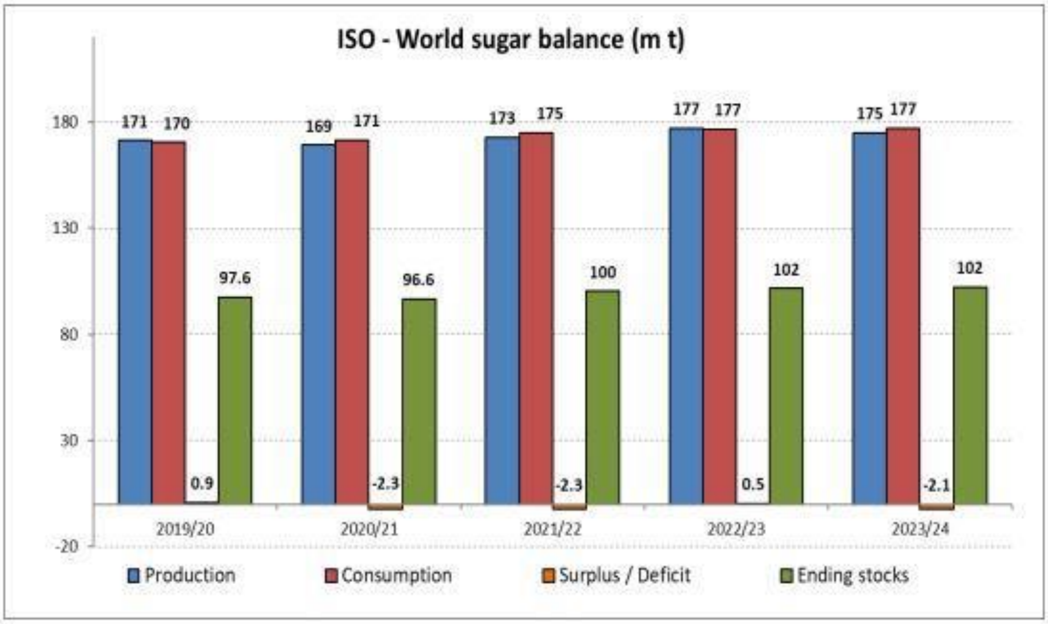

Fig. 1. World sugar balance [6].

Beet sugar is produced from the roots of sugar beets – wedge-shaped, white tubers. Beetroots collected from the field are cleaned of soil residues and other impurities. After washing the tubers, the beets are cut into small pieces. Small pieces of sugar beets go to a device called a diffuser, which, thanks to water at an elevated temperature of 75-850C, leaches sugar. This process allows you to obtain sweetened slivers and beetroot juice, which can contain up to 15% sugar. The juice obtained in this way is sent to further stages of production. The liquid is subjected to filtration and refining processes. Then the purified beetroot juice is boiled and evaporated several times. The last stage of sugar production is centrifuging the juice, which allows for the production of sugar crystals – Fig. 2. However, in addition to sugar crystals, a by-product is created in the form of molasses. It contains 40-50% sucrose, which cannot be converted into crystals. Therefore, molasses is used in the food industry as a sugar substitute. It can be used to produce alcohol, bakery or feed yeast, but also to produce glycerin and organic acids (citric and oxalic). It is also a rich source of non-heme iron, and betaine can also be isolated from molasses, which improves the blood lipid profile and supports fat metabolism in the liver [7].

We should also not forget about the antioxidant properties of molasses, which are the pigments that give it its dark brown color. Antioxidant properties mean that molasses has anti-inflammatory, antibacterial and anticancer effects, supports the immune system, and reduces the risk of circulatory system diseases. Comparative studies of the antioxidant properties of honey and molasses have shown that molasses has them 60 times greater (in the case of beet molasses) and 200 times greater (in the case of cane molasses) than honey [9-12].

It is worth adding here that the entire sugar beet plant is a source of bioactive molecules with a potential cardioprotective and vascular role.

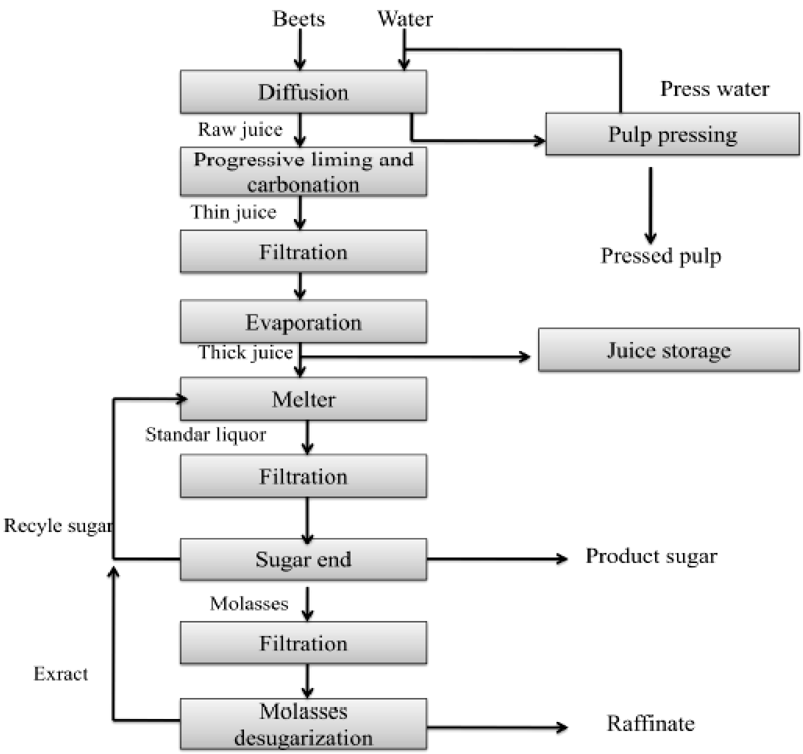

Fig. 2. Beet sugar production process [8].

Betaine and B vitamins from the leaves and crown are involved in homocysteine detoxification and NO synthesis, respectively. Nitrates, betalains and phenolic compounds from the beet pulp, and its byproduct molasses, are involved in NO bioavailability, glycemic control and reduction of oxidative stress and inflammation. In addition, fibers from different parts of the plant have hypoglycemic and cholesterol-lowering effects – Fig. 3.

Due to the wide range of uses of molasses, knowledge of its flow behavior is useful in engineering applications related to the proper design and operation of units and can also help in understanding its transport processes. The rheological properties of molasses are therefore an important factor influencing the performance of various sugar production and refining processes such as cooking, crystallization, centrifugal separation and pumping.

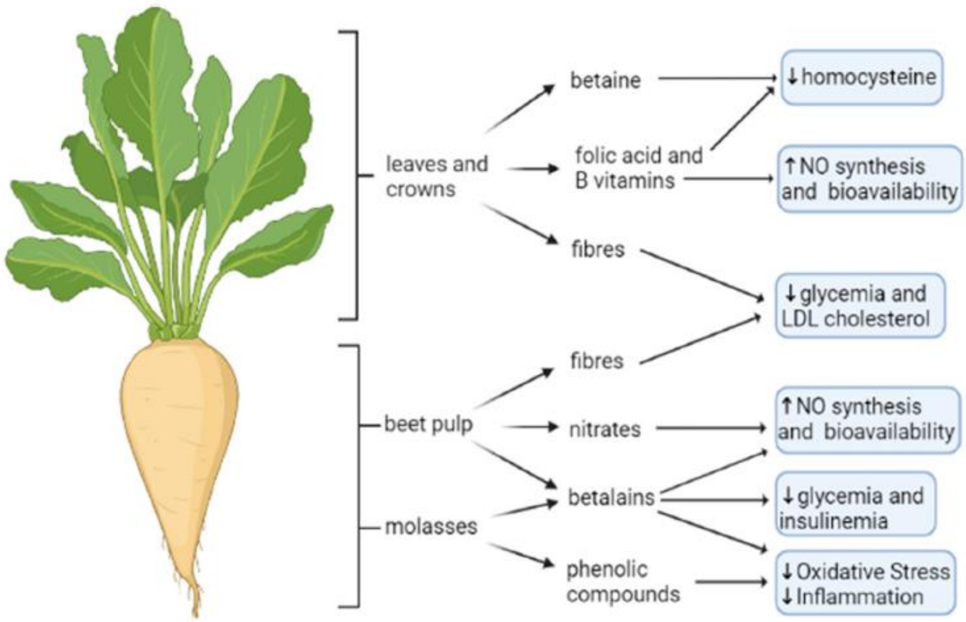

Fig. 3. Sugar beet bioactive compounds and their cardio- and vasculoprotective actions [13].

Moreover, knowledge of the rheological properties of molasses is important because it provides us with information about its physical properties and helps in understanding the mechanisms underlying momentum and heat transfer. In the feed industry - molasses is also an additive to animal feeds e.g. horses - viscosity is one of the most important parameters required in the process design for mixing feed and molasses [14].

Therefore, the aim of the presented work is to assess the rheological properties of molasses obtained as a by-product during the production of table sugar in one of the Polish sugar factories and to compare its properties with the properties of molasses from foreign sugar factories.

2. Materials and Methods

The research material was molasses, a waste product from the production of table sugar in the Polish sugar factory in Glinojeck – Fig. 4.

Fig. 4. Molasses from the Polish sugar factory in Glinojeck in powder and liquid form [own materials].

The rheological properties of the raw molasses sample were determined using a Physica MCR 301 rotational rheometer from Anton Paar in a cone-plate measuring system with a cone diameter of 50mm, an inclination angle of 1^0 and a distance between the measuring elements, i.e. the cone and the plate, of 0.048mm.

Rheological tests were carried out consisting in measuring the viscous properties of the obtained raw molasses sample in the shear rate range from 1 to 100s^{-1}, i.e. in the range of two logarithmic decades, taking 8 measurement points for each decade of shear rate. The tests were carried out in the temperature range from 40^0C to 60^0C, taking measurements every 5^0C.

A sample of the obtained raw molasses was placed in the measuring system of the rotational rheometer and left at rest for 30 minutes at a constant temperature to achieve thermal and mechanical equilibrium.

To describe the flow and viscosity curves obtained from rheometric measurements, the Ostwald de Waele power law model of the form [15] was used:

$$\tau = k \cdot \gamma^n \qquad (1)$$

$$\eta = k \cdot \gamma^{n-1} \qquad (2)$$

where the rheological parameters of this model are:

n – the flow behavior index, [-],

k – the flow consistency index, [$Pa \cdot s^n$]

Mathematical analysis concerning the determination of rheological parameters of the Ostwald de Waele model was carried out using nonlinear regression methods from Excel. One of the tools of this program, namely the Solver add-on, was used to solve the mathematical modeling task, i.e. to find such parameters of the mathematical model that would best describe the tested raw molasses sample.

In order to assess the correctness of the description of experimental data using the Ostwald de Waele model equation, a statistical assessment of the fit of the model curves to the experimental curves was carried out, related to the value of the shear stress τ obtained directly from rheometric measurements. This assessment was made by estimating the modeling efficiency R^2. The Ostwald de Waele power model is one of the simplest and most commonly used rheological models. It was selected to assess the rheological properties of raw molasses in order to relate the obtained results to the literature data. The literature data consisted of published studies on the rheological properties of raw molasses samples obtained from a sugar factory in Bač (Serbia) [16] and from a sugar factory in Elaziğ (Turkey) [17].

3. Results and Discussion

The graphs in Fig. 5 and Fig. 6 show, respectively, the flow curves and viscosity curves of the tested sample of Polish raw molasses in the temperature range from 40^0C to 60^0C compared to such curves for samples of raw molasses from Serbia and Turkey in a comparable temperature range. Table 1 shows the parameters of the Ostwald de Waele model for the analyzed molasses.

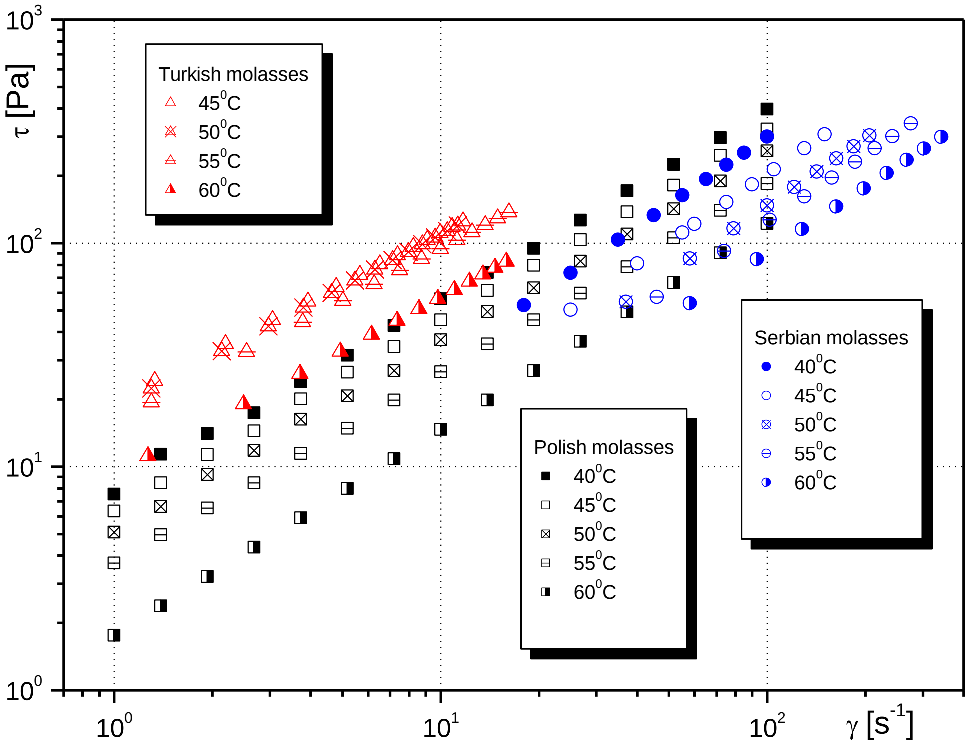

Fig. 5. Flow curves of Polish, Serbian and Turkish raw molasses.

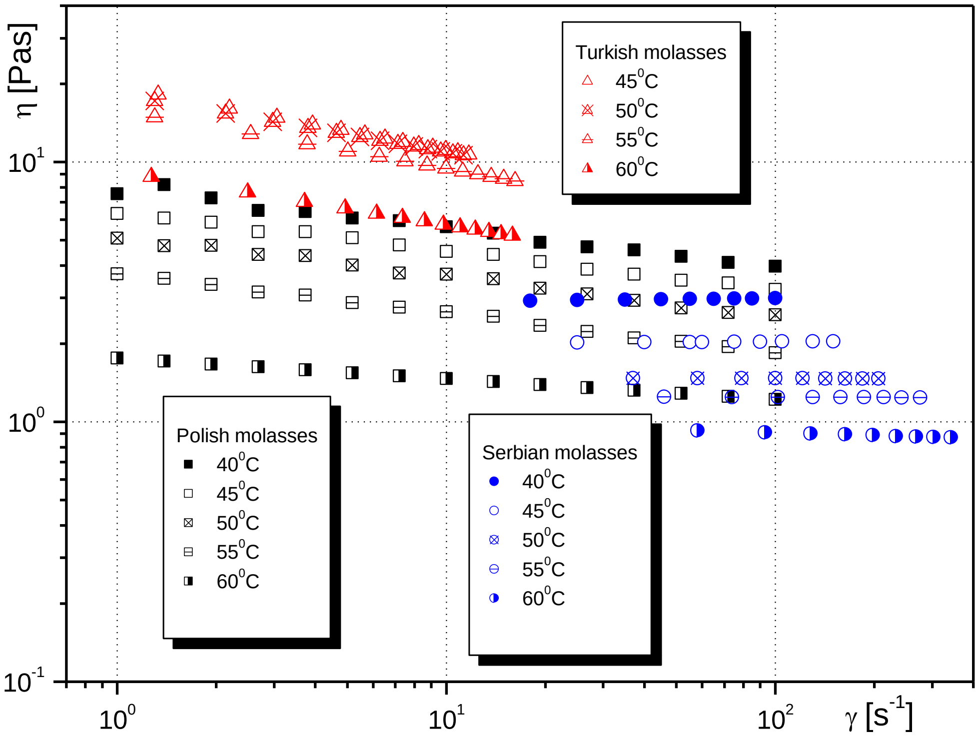

Fig. 6. Viscosity curves of Polish, Serbian and Turkish raw molasses.

Analysis of the obtained experimental data presented in Fig. 6 allowed us to state that the viscosity of raw molasses from the sugar factory in Bač (Serbia) remains at a constant level in the entire analyzed range of shear rates. This allows us to state that raw Serbian molasses is a Newtonian fluid, which is also indicated by the parameter of the power model, the flow behavior index n, the value of which oscillates around 1 – Tab. 1.

Tab. 1. Rheological parameters of the Ostwald de Waele power-law model.

Raw molasses	**40 [^{0}C]**	**45 [^{0}C]**	**50 [^{0}C]**	**55 [^{0}C]**	**60 [^{0}C]**
Polish molasses from Glinojeck					
n[-]	0.848	0.851	0.856	0.869	0.921
K [Pas^n]	7.889	6.407	5.166	3.728	1.759
R^2	0.999	0.999	0.999	0.998	0.998
Serbian molasses from Bač					
n[-]	1.013	1.007	0.998	0.997	0.965
K [Pas^n]	2.820	1.973	1.485	1.263	1.068
R^2	0.999	0.999	0.999	0.999	0.999
Turkish molasses from Elaziğ					
n[-]	-	0.756	0.777	0.776	0.793
K [Pas^n]	-	19.510	18.240	15.810	9.230
R^2	-	0.998	0.999	0.996	0.991

In the case of raw molasses from a sugar factory in Elaziğ (Turkey), the flow curves shown in Fig. 6 show that the viscosity of Turkish molasses clearly decreases with increasing shear rate. Therefore, the Turkish raw molasses is a shear-thinning non-Newtonian fluid. This is confirmed by the values of the parameter n of the power model, which ranges from 0.756 for a temperature of 45^{0}C to 0.793 for a temperature of 60^{0}C – Table 1.

Viscosity curves - Fig. 6 - of raw molasses from a sugar factory in Glinojeck (Poland) indicate that it is also a non-Newtonian fluid thinned by shear, because its viscosity decreases with increasing shear rate in the entire analyzed temperature range. The flow behavior index, i.e. parameter n of the power model for Polish raw molasses, takes values from 0.848 for a temperature of 40^{0}C to 0.921 for a temperature of 60^{0}C - Table 1. It should be noted, however, that the values of parameter n of the power model of molasses from Poland are about 0.1 higher than those of Turkish molasses.

The highest viscosity values are definitely characteristic of molasses from Elaziğ (Turkey) – Fig. 6. The viscosity of this molasses decreases by half only at a temperature of 60^0C. It is interesting that the viscosity values of Turkish molasses at 60^0C correspond to the viscosity values of Polish molasses, but at 40^0C. Therefore, Polish molasses from Glinojeck at a temperature of 40^0C has properties similar to Turkish molasses from Elaziğ at 60^0C – this is also indicated by the value of the consistency coefficient k of the power model – Tab.1.

The data presented in the graph in Fig.6 also show that the lowest viscosity value was recorded for molasses from Bač (Serbia) at a temperature of 60^0C. The viscosity values of Serbian molasses at temperatures below 60^0C correspond to those of Polish molasses from Glinojeck. For example, molasses from Bač (Serbia) at a temperature of 40^0C has a viscosity corresponding to the viscosity value of Polish molasses from Glinojeck at a temperature of 50^0C. However, this occurs in the range of slightly higher shear rate values, i.e. in the second logarithmic decade.

Based on the presented data - shown in Fig. 5 and 6 and in Table 1 - it can be stated that the structure of Serbian molasses from Bač seems to be more resistant to shear damage, because its viscosity remains at a certain constant level with increasing shear rate at each of the analyzed temperatures. Meanwhile, the viscosities of Turkish molasses from Elaziğ and Polish molasses from Glinojeck (although higher in value than molasses from Bač) decrease with increasing shear rate. Therefore, the structure of both these molasses - Polish and Turkish - in the studied temperature range is probably more susceptible to shear damage than molasses from Bač.

4. Conclusions

The composition of molasses, as well as its consistency, depend on the quality and chemical composition of the raw material, i.e. sugar beet. They also depend on the technological process, i.e. on the method of obtaining sugar from sugar beets, and finally, they depend on the storage conditions of the raw material itself. Molasses is used in the food industry as a sugar substitute, because it contains 40-50% sucrose, which can no longer be converted into crystals. The basic issue that determines the amount of sucrose in sugar beet is its variety, as well as the growing conditions - including temperature and amount of rainfall. These conditions, in turn, depend on the geographical location, which is significantly different for each of the molasses analyzed here. Thus, with moderate soil moisture and on sunny, warm days, sugar beets are able to store a larger amount of sucrose.

However, as Baryga points out in his work [18], determining the sucrose content is not easy, because the use of different analytical procedures can cause significant differences in the obtained results of the sucrose content in sugar beet. The authors of this article, without knowing the sucrose content in the analyzed material, as well as the variety of sugar beet from which molasses was obtained after processing, and such data were not included in the works of Popović [16] and Toğrul [17], are not able to state at this stage what the possible similarities and differences presented in the presented comparative analysis of the mentioned molasses result from. Due to the fact that the rheological properties of molasses are an important factor influencing the efficiency of various production processes, knowledge of this data seems necessary.

References

[1] Kirk D.E., Othmer D.F.: *Molasses*, Encylopedia of chemical technology, 13, pp. 613-632, 2nd ed. John Wiley and Sons, New York (1967).

[2] Kumar R., Jain V.K., Sayed V.K., Sajid A.S., Sanyal P.: *Rheological behavior of Indian cane molasses*. International Sugar Journal, 96, 1994, pp. 124–127.

[3] Kaur S., Kaler R.S.S., Aamarpali A.: *Effect of starch on the rheology of molasses.* Journal of Food Engineering, 55, 2002, pp. 319–322.

[4] Melani J.M., Naghavi E.A., Golkar A., Khosravi T.: *Rheological behavior of different phases of grape molasses after storage: Effect of concentration and temperature.* J Food Process Preserv. 43, 2019, e14013.

[5] Karaman S., Kayacier A.: *Effect of temperature on rheological characteristics of molasses: Modeling of apparent viscosity using Adaptive Neuro e Fuzzy Inference System (ANFIS).* LWT - Food Science and Technology 44, 2011, pp. 1717-1725.

[6] Chylińska A.: *Rynek cukru.* Ministerstwo Rolnictwa i Rozwoju Wsi, Departament Rynków Rolnych, Warszawa (2023).

[7] Kołożyn-Krajewska D., Sikora T.: *Towaroznawstwo żywności*. WSiP, Warszawa (2007).

[8] Rafik M., Qabli H., Belhamidi S., Elhannouni F., Elkhedmaoui A.,. Elmidaoui A.: *Membrane separation in the sugar Industry*, Journal of Chemical and Pharmaceutical Research 7, 2015, pp. 653-658.

[9] Guimaraes C.M., Giao M.S., Martinez S.S., Pintado A.I., Pintado M.E., Bento L.S., Malcata F.X.: *Antioxidant Activity of Sugar Molasses, Including Protective Effect Against DNA Oxidative Damage.* Journal of Food Science 72, 2007, pp. 39-43.

[10] Valli V., Gómez-Caravaca A.M., Di Nunzio M., Danesi F., Caboni M.F., Bordoni A.: *Sugar Cane and Sugar Beet Molasses, Antioxidant-rich Alternatives to Refined Sugar.* Journal of Agricultural and Food Chemistry 60, 2012, pp. 12508−12515.

[11] Šarić L.Ć., Filipčev B.V., Šimurina O.D., Plavšić D.V., Šarić B.M., Lazarević J.M., Milovanović I.L.: *Sugar beet molasses: properties and applications in osmotic dehydration of fruits and vegetables.* Food and Feed Research 43, 2016, pp. 135-144.

[12] Filipčev B., Mišan A., Šarić B., Šimurina O.: *Sugar beet molasses as an ingredient to enhance the nutritional and functional properties of gluten-free cookies.* International Journal of Food Sciences and Nutrition 67, 2016, pp. 249-256.

[13] Caliceti C., Malaguti M., Marracino L., Barbalace M.C., Rizzo P., Hrelia S.: *Agri-Food Waste from Apple, Pear, and Sugar Beet as a Source of Protective Bioactive Molecules for Endothelial Dysfunction and Its Major Complications.* Antioxidants 11, 2002, pp. 1786-1810.

[14] Steffe J.F.: *Rheological methods in food process engineering.* East Lansing MI: Freeman Press (1992).

[15] Dziubiński M., Kiljański T., Sęk J.: *Podstawy reologii i reometrii płynów*. Wydawnictwo Politechniki Łódzkiej, Łódź (2009).

[16] Popović S., Lević L., Paunović R., Mišljenović N., Koprivica G.: *Viscosity Change Of Sugar Beet Molasses While Adding Starch.* Biblid. 13, 2009, pp. 320-323.

[17] Toğrul H., Arslan N.: Mathematical model for prediction of apparent viscosity of molasses. Journal of Food Engineering 62, 2004, pp. 281-289.
[18] Baryga A.: Czynniki wpływające na zawartość sacharozy w burakach cukrowych i wyniki jej oznaczania. Poradnik Plantatora Buraka Cukrowego 1, 2021, pp. 16-18.

Correlation analysis of the relationship between the structural parameters of fabrics and the parameters characterizing the geometric structure of the fabric surface

Gabriela Kosiuk[1,2]*, Małgorzata Matusiak[2]

[1] Institute of Security Technologies MORATEX, Lodz, Poland
[2] Lodz University of Technology, Faculty of Material Technologies and Textile Design, Institute of Architecture of Textiles, Lodz, Poland

Abstract

The geometric structure of the surface of textile materials has a very important functional, operational and aesthetic significance. Generally, the geometric structure of surface consists of three components: shape, waviness and roughness. Textile materials, such as woven fabrics, knitted fabrics or nonwovens, are flexible materials, and therefore, with some exceptions, the shape of their surface is not discussed or determined. It is assumed that their surface is mostly flat. Roughness is one of the surface quality features most often assessed using quantitative indicators, called surface roughness parameters. The aim of the presented research is to analyse the correlation between selected parameters characterizing the geometric structure of surface of the cotton woven fabrics and the structural parameters of the fabrics. Surface topography measurements were performed using the MicroSpy® Profile profilometer from FRT the art of metrology™. The correlation analysis was carried out using the TIBCO Statistica software, version 13.3. Obtained results showed that there is a correlation between the structural parameters and the surface geometry parameters of the fabrics. However, the strength of these relationships varies and sometimes is not too high.

Keywords: woven fabrics, roughness, surface, structure, correlation, profilometer

1. Introduction

Surface quality is one of the characteristics of all kinds of objects. The surface is a kind of coating that “covers” the interior of the object, separating the object

* corresponding author e-mail: g.kosiuk@gmail.com
DOI: 10.57636/69.2024.1.3

from its surroundings. The surface of an object determines its appearance, as well as its interaction with other objects and media surrounding the object, such as fluids or gases. The surface characteristic is a very important feature of textile materials. Unlike other objects, textile materials come into contact with the human body, especially the skin. This is due to the fact that one of the most important applications of textile materials is clothing. The properties of clothing are shaped mainly by the selection of appropriate materials. Especially, in the case of clothing that is worn next to user's skin, the surface properties, including the geometric structure of the material surface, can play a crucial role. It influences such functions and performance of clothing as: light reflectance, thermal radiation, thermal resistance, wettability, tactile features, abrasion resistance and of course the clothing appearance [1 – 4].

The most common and recognized method of measuring the roughness of textile materials is the contact/stylus method used in the KES (Kawabata Evaluation System) FB4 module. The instrument measures the roughness of surface of textile materials by the profile method measuring the surface irregularities along the line, separately in the warp and weft direction. This device provides information on the value of only one parameter characterizing the surface quality of textile materials – SMD (Surface Mean Deviation) [5, 6]. It is the equivalent of the arithmetic mean of the ordinates of the roughness profile R_a, which is commonly called roughness. Like any average, the R_a parameter can take the same value for diverse sets of individual values. Therefore, scientists dealing with the issues of geometric structure of the surface believe that the R_a parameter does not fully characterize the surface topography. With the same R_a value, you can deal with a very diverse surface geometry. In addition, contact tests do not fully reflect the shape of the tested surface, because surface irregularities smaller than the dimensions of the measuring sensor are not recorded. It is also important to note, that textile materials are flexible. They can be deformed by the sensor sliding across the surface of the fabric. All above factors are disadvantages of the contact methods of surface geometry measurement.

Contactless optical methods are much more precise than contact methods. In addition, contactless methods provide information on a number of parameters and functions that comprehensively describe the geometric structure of the surface. They are:

- the amplitude parameters such as: maximum height (R_z), maximum profile peak height (R_p), maximum profile valley depth (R_v), mean height (R_c) and total height (R_t),
- amplitude average parameters: arithmetic mean deviation (R_a), root mean square deviation (R_q), skewness (R_{sk}), kurtosis (R_{ku}),
- hybrid parameters,
- material ratio curve and related parameters: material ratio ($R_{mr(c)}$), profile section height difference (R_{dc}), relative material ratio (R_{mr}),
- parameters of surface having stratified functional properties: core roughness depth (R_k), reduced peak height (R_{pk}), reduced valley depth (R_{vk}), material portion (Mr_1) and (Mr_2).

Particular parameters: amplitude, hybrid and derived from the material curve are defined in the ISO 4287:1996 standard [7] whereas, the parameters form the last group are standardised in the ISO 13565-2:1996 standard [8]. Which of these parameters are important depends on the object being examined, its purpose and desired properties. In the field of textile materials, knowledge on this subject is very limited. A number of studies of surfaces of the textile materials using non-contact methods have already been published, but these were rather case studies, focused on assessing the method used, selecting filters, or assessing a specific textile product [9 – 11].

The aim of presented work was to analyse the relationships between the structure of the cotton woven fabrics and their surface geometry parameters. In order to do it 21 cotton fabric variants were measured in the range of their surface geometry using the contactless optical method. The fabrics were characterized by different and intentionally diversified structure. The structural parameters of the investigated fabrics were measured using the standardized methods. Correlation analysis allowed to assess the relationship between the structural parameters of the investigated cotton woven fabrics and their surface geometry parameters.

2. Material and Methods

The woven fabrics of different structure have been the objects of the investigations. There were 21 variants of fabrics made of cotton. The fabrics were produced on the basis of the same warp – 50 tex CO OE (Open End), warp density – 32/cm. The fabric were manufactured in six weaves: plain, twill 1/1 S, twill 2/2 S, rep 1/1 (010), rep 2/2 (2) and hopsack 2/2(020) using two kinds of weft yarn: 60 tex CO OE and 100 tex CO OE. Additionally the weft density was changed. The fabrics were finished in the same way using standard cotton finishing: dyeing, washing and drying. The basic parameters of the cotton woven fabrics being analysed are presented in Table 1.

Tab. 1. The basic properties of the investigated woven fabrics

Fabric variant	**Weave**	**Weft yarn tex**	**Warp density cm^{-1}**	**Weft density cm^{-1}**	**Mass per square meter, g/m^2**	**Thickness mm**
1.	plain	100	31.2	11.5	292	0.67
2.	plain	60	31.6	11.7	240	0.59
3.	plain	100	31.4	9.36	269	0.69
4.	plain	100	31.4	7.32	242	0.71
5.	twill 3/1 S	100	31.5	7.36	241	0.80
6.	twill 3/1 S	100	31.8	9.4	266	0.79
7.	twill 3/1 S	100	31.7	11.6	292	0.78

8.	twill 3/1 S	60	31.7	11.7	238	0.74
9.	twill 3/1 S	50	31.7	11.6	225	0.67
10.	twill 3/1 S	50	32	11.8	228	0.71
11.	twill 3/1 S	40	32	11.8	215	0.65
12.	twill 3/1 S	30	31.8	11.8	198	0.61
13.	twill 3/1 S	30	31.6	11.6	187	0.57
14.	twill 2/2 S	100	31.9	11.6	287	0.79
15.	twill 2/2 S	60	31.9	11.8	238	0.76
16.	rep 1/1 (010)	100	31.1	11.5	284	0.83
17.	rep 1/1 (010)	60	31.7	11.8	237	0.78
18.	rep 2/2 (2)	100	31.7	11.9	293	0.65
19.	rep 2/2 (2)	60	32.0	11.8	242	0.60
20.	hopsack 2/2 (020)	100	31.6	11.7	287	0.79
21.	hopsack 2/2 (020)	60	31.6	11.7	234	0.76

The measurement of basic structural parameters was done using the standardised methods:

- mass per square meter – according to the PN-EN 29073-1:1994,
- warp and weft density – according to the PN-EN 1049-2:2000,
- fabric thickness – according to the PN-EN ISO 5084:1999.

The measurement of the parameters characterizing the surface geometry of the investigated woven fabric was performed by means of the contactless method using the MicroSpy® Profile profilometer (Fig. 1) by the FRT® the art of metrology™ [12 – 14].

Fig. 1. MicroSpy® Profile profilometer

It is the optical method for the precise measurement of the surface characteristic using the principle of chromatic distance measurement. The instrument uses a non-contact optical scanning method to generate 3D images of surface topography with submicron resolution. The instrument is equipped with a confocal microscope that focuses a beam of white light on the sample surface and measures the reflected light to determine the height and shape of surface features. The profilometer is equipped with a CWL sensor, which is based on a patented method using chromatic aberration of optical lenses. The profilometer cooperates with the FRT Mark III software for calculation of numerous surface parameters according to standards [7, 8, 15]. The scan of fabric sample was done for the square area with a side of 49 mm. For each fabric variants ten repetition of measurement was performed for samples taken from different area of the fabric. The exemplary scan of fabric surface obtained from the profilometer is presented in Fig. 2.

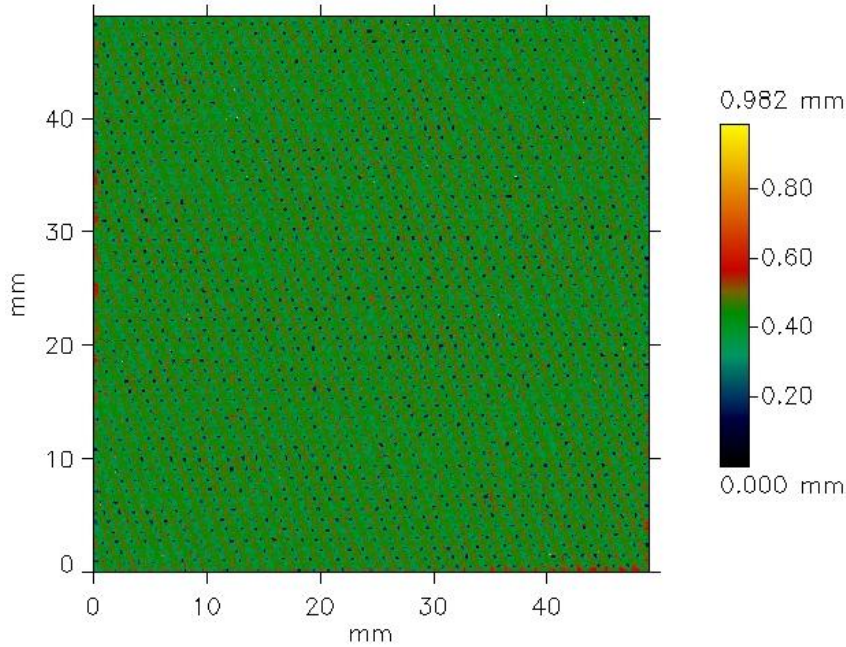

Fig. 2. The exemplary scan of the woven fabric obtained from the profilometer

In the presented work, on the basis of the data from the profilometer processed by the Mark III software the parameters and functions characterizing the surface geometry of fabrics were calculated according to the ISO 4287:1996 standard [7].

Next, the correlation analysis was performed using the TIBCO Statistica software. The correlation relationships between the parameters of surface geometry of the investigated woven fabrics and their structural parameters were analysed.

3. Results and Discussion

The values of the correlation coefficients between the parameters characterising the surface geometry of the investigated cotton woven fabrics and their structural parameters are presented in Table 2. In the table the statistically significant relationships at the significance level 0.05 are marked by red.

Tab. 2. The values of the correlation coefficients between the surface geometry parameters of the woven fabrics and their structural parameters

Surface parameter	The value of correlation coefficient					
	m	**g_1**	**g_2**	**W_1**	**W_2**	**h**
Ra	-0.0919	-0.0842	-0.3053	-0.2530	-0.5930	0.7778
Rq	-0.0759	0.0004	-0.3018	-0.2774	-0.5350	0.7804
Rz	-0.1229	0.0893	-0.3047	-0.0459	-0.0874	0.1770
Rp	0.1223	0.1074	-0.3107	-0.0001	-0.1152	0.2978
Rv	-0.1891	-0.1439	-0.4101	-0.2166	-0.1193	0.1450
Rt	-0.1859	0.0068	-0.3855	0.1715	-0.1011	0.3275
Rsk	0.4536	-0.3847	0.1286	0.2606	-0.0259	-0.4234
Rku	0.0326	0.3351	0.2085	0.1891	0.6467	-0.4821
Rk	0.1954	-0.5089	-0.2183	0.3360	-0.5744	0.5197
Rpk	0.3982	-0.4022	-0.1418	0.1212	-0.6819	0.6490
Rvk	-0.1741	0.0993	-0.4988	-0.3811	-0.1155	0.4336
Mr1	-0.0359	0.2916	0.0245	-0.1563	0.3676	-0.3942
Mr2	0.3371	-0.4747	-0.0460	0.6673	-0.1050	-0.0287
Rmr(c)	-0.0946	-0.1287	0.2693	0.0494	0.0586	-0.2650

In the Table 2 the following symbols of fabrics' structural parameters are applied:

m – mass per square meter.

g_1 – density of warp,

g_2 – density of weft,

W_1 – take-up of warp,

W_2 – take-up of weft.

h – fabric thickness.

Based on the correlation analysis, it was found that there is statistically significant correlation between some basic parameters of fabric structure and individual roughness parameters determined using a profilometer. The R_a and R_q parameters are considered as the basic surface roughness parameters (Fig. 3 and Fig. 4). They are the most commonly determined and analysed. The R_a parameter is defined as an arithmetic mean of the absolute height (ordinate z) within the sampling length or area. The R_q parameter represents the root mean square for z-value (height of particular points on the measured surface) within the sampling length or area. It was stated that the statistically significant correlation exists between both mentioned surface parameters R_a and R_q and fabric thickness – values of correlation coefficients are respectively: 0.7778 and 0.7804.

Fabric thickness is also correlated with other parameters characterizing the geometry of the fabric surface: R_{ku}, R_k, R_{pk} and R_{vk}. R_{ku} - kurtosis is a parameter, which relates to the tip geometry of peaks and valleys and is suitable for analysing the degree of contact between two objects. $R_{ku} = 3$ means a normal distribution of height on the measured surface, R_{ku} greater than 3 means that the height distribution is sharp whereas, R_{ku} lower than 3 informs that the height distribution is even. The relationship between the fabric thickness and kurtosis is negative. It means that the greater thickness is the lower value of the kurtosis. It should be mentioned that for all investigated fabrics the value of kurtosis is greater than 3 (Fig. 5). It means that the height distribution on fabrics' surface is sharp.

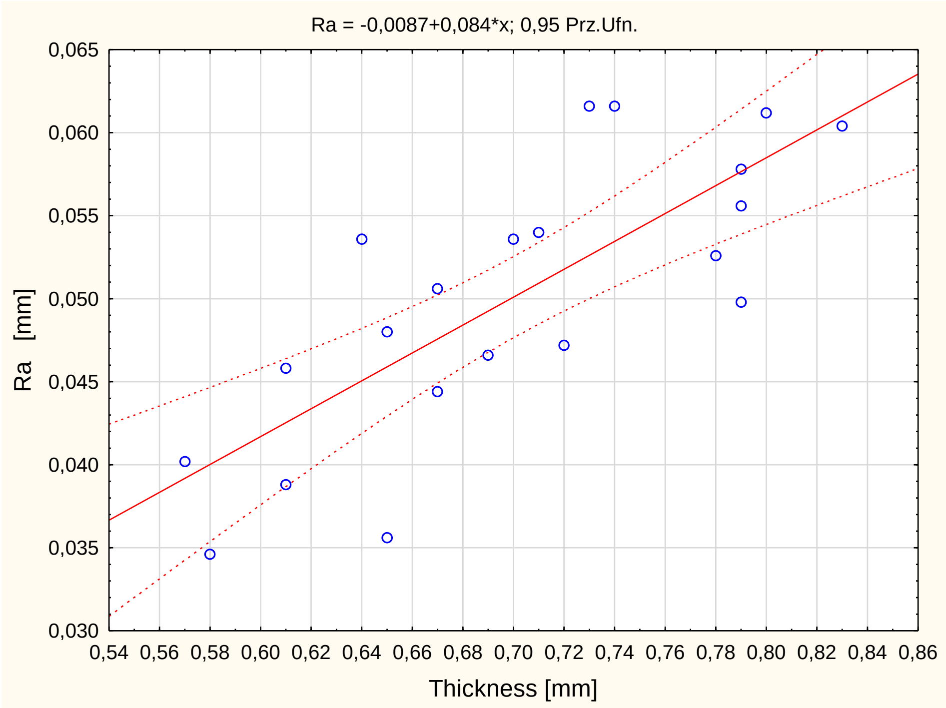

Fig. 3. Relationship between the R_a parameter and fabric thickness

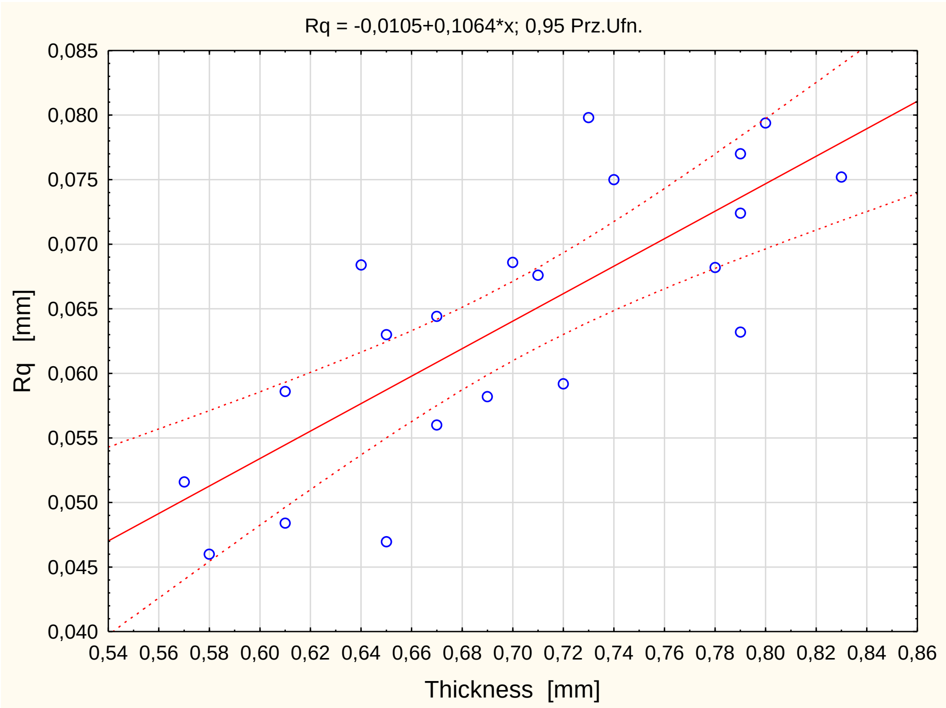

Fig. 4. Relationship between the R_q parameter and fabric thickness

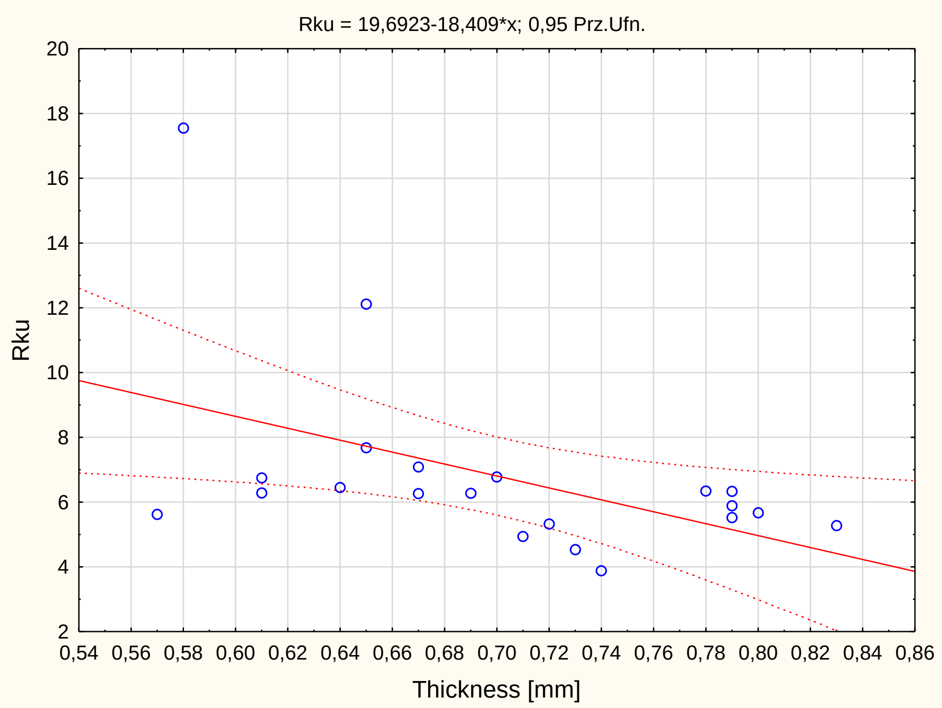

Fig. 5. Relationship between the R_{ku} parameter – kurtosis and fabric thickness

Also in the case of the W_2 structural parameter – take-up of weft yarn there are some relationships with the surface geometry parameters. The positive and statistically significant relationship occurs between the weft take-up and kurtosis, the negative relationships are observed between the weft work-up and R_{pk} (Fig. 6), R_k, R_a and R_q surface parameters. The R_{pk} means the reduced peak height on the measured surface whereas, the R_k is a core roughness depth. Both parameters are derived from the material ratio curve.

It was also stated that there is statistically significant correlation between the take-up of warp yarn and the M_{r2} surface parameter (Table 2). The M_{r2} is also derived from the material ration curve. Above results indicate that the material ratio curve can be of significant importance in the analysis of the geometric structure of fabric surfaces. It shows that it is advisable to analyse deeply the material ratio curve and the parameters derived from it in the analysis of fabric surface geometry and an assessment of the relationship between surface geometry and fabric properties.

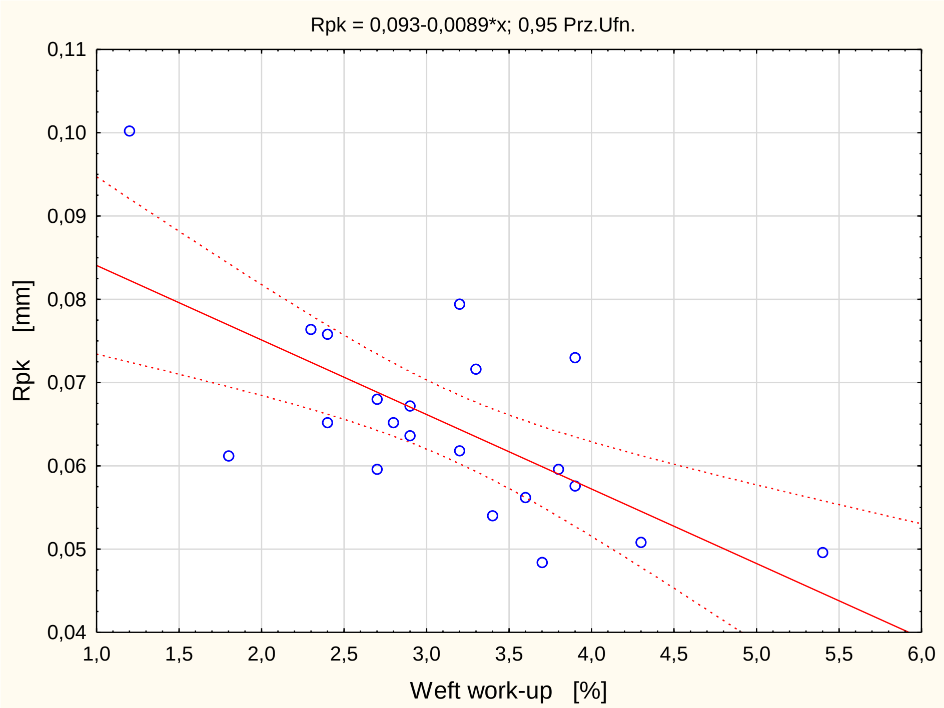

Fig. 6. Relationship between the R_{pk} parameter and work – up the weft yarn

It should be mentioned here that the values of correlation coefficients presented in the Table 2 are note very high. The results are surprising because it was expected that the relationships between the structural parameters of the woven fabrics and surface geometry parameters are stronger. It was not confirmed. Low values of correlation coefficients between fabric structure parameters and parameters characterizing the geometric structure of fabrics' surface result from the fact that the geometry of fabric surface is shaped by many factors connected with the fabrics structure. None of these factors is dominant. There is also an interaction between the fabric structural parameters, which affects their influence on the geometric structure of fabric surface.

4. Conclusions

On the basis of the performed investigations it was stated that it is possible to characterize the surface geometry of the woven fabrics in a complex way using contactless optical method. The MicroSpy® Profile profilometer cooperating with the Mark III software provides a wide range of parameters which can be connected with structural and functional properties of the woven fabrics. Obtained results showed that there is correlation between some structural parameters of the cotton woven fabrics, especially thickness and weft take-up and parameters characterising the geometry of surface of the fabrics. However, the correlation is not very strong. It can be due to the fact that the surface of the woven fabrics is shaped by several structural factors which interact between each other.

It is necessary to continue the investigation, for instance in direction of better understanding the material ratio curve and parameters derived from it in order to better characterisation of surface of textile materials as well as to analyse the relationships between the surface geometry of fabrics and their performance.

References

[1] Hasan M.M.B., Calvimontes A., Synytska A., Dutschk V.: *Effects of Topographic Structure on Wettability of Differently Woven Fabrics*, Textile Research Journal 2008, 78; 996

[2] Sahoo P.: *Surface topography*, In: Tribology for Engineers. A Practical Guide, ed. Davim J.P., Wodhead Publishing Ltd. Cambridge England 2011, pp. 1-39

[3] Adamczak S., *Pomiary geometryczne powierzchni. Zarys kształtu, falistość, chropowatość,* WNT Warszawa 2008

[4] Kurpanik R., Rogowska P., Sarraj S., Walke W.: *Wpływ przygotowania powierzchni oraz parametrów procesu utleniania anodowego na zwilżalność i odporność korozyjną tytanu* CPTI GRADE 2, Aktualne Problemy Biomechaniki, nr 18, 2019, pp. 5-12.

[5] Krucińska I., Konecki W., Michalak M., *Systemy pomiarowe we włókiennictwie*. Wydawnictwo Politechniki Łódzkiej, Łódź 2006, pp. 252-329.

[6] Matusiak M., Bajzik V., *Badania właściwości powierzchniowych tkanin gofrowanych*. In: Tkaniny gofrowane. Właściwości mechaniczne, ed. Matusiak M., Frączczak Ł., Wydawnictwo Politechniki Łódzkiej, Łódź 2021, pp. 243-282.

[7] ISO 4288:1996 Geometrical product specifications (GPS) - Surface texture: Profile method - Rules and procedures for the assessment of surface texture.
[8] ISO 13565-2:1996 Geometrical Product Specifications (GPS) — Surface texture: Profile method; Surfaces having stratified functional properties. Part 2: Height characterization using the linear material ratio curve.
[9] Matusiak M.*, Investigation of Surface Geometry of Seersucker Woven Fabrics,* Autex Research Journal, l, Vol. 23, No. 3, 2023, pp. 409-419.
[10] Mooneghi, S. A., Saharkhiz, S., Varkiani, M. H.: *Surface roughness evaluation of textile fabrics: a literature review*. Journal of Engineered Fibers and Fabrics 9(2), 2014, pp. 1–18.
[11] Semnani, D., Hasani, H., Behtaj, S., Ghorbani, E.: *Surface roughness measurement of weft knitted fabrics using image processing*. Fibres and Textiles in Eastern Europe, 19, 3(86), 2014, pp. 55–99.
[12] Operating Manual FRT MicroSpy® Profile, Version 2.104, FRT the art of metrology™, Bergisch Gladbach, Germany, 2016.
[13] Matusiak M.: *Application of profilometric measurements in an assessment of woven fabrics surface geometry*, Journal of Natural Fibres, Vol. 21. Is. 1, 2024, 2293048.
[14] Matusiak M.: *Wpływ efektu gofrowania na wybrane właściwości tkanin gofrowanych*, Technologia i Jakość Wyrobów, 66, 2021, pp. 46-64.
[15] Manual Mark III, Version 3.11.FRT the art. of metrology™, 2018

Identifying the needs for specialist clothing for children with disabilities

Małgorzata Matusiak[1]* Karolina Serafin[2], Magdalena Kłonowska[3]

[1*] Lodz University of Technology, Faculty of Material Technologies and Textile Design, Institute of Architecture of Textiles, Lodz, Poland
[2] Lodz University of Technology, Faculty of Material Technologies and Textile Design, Lodz, Poland
[3] Lodz University of Technology, Facultu of Material Technologies and Textile Design, Textile Institute, Lodz, Poland

Abstract

With the development of civilization, people's needs in terms of clothing and the possibilities of satisfying them have developed. Today, clothing can fulfil functions of monitoring the vital functions of the user's body or therapeutic functions. The latter consist in supporting therapy or prevention of many health problems. As part of the work, surveys were conducted to identify the needs of children with disabilities in terms of specialist clothing. The research was conducted among parents and guardians of children with disabilities. The results allowed for the identification of problems related to the use of clothing by children with disabilities and the proposal of solutions that can improve the quality of life of these children and their guardians.

Keywords: therapeutic clothing, comfort, analysis of needs, children, disability

1. Introduction

Clothing is present in the life of every person from birth through all next stages of life. There are many different product groups of clothing meeting different requirements [1, 2]. The basic – primary functions of clothing include:

- organizational functions,
- protective functions,

* corresponding author e-mail: malgorzata.matusiak@p.lodz.pl.
DOI: 10.57636/69.2024.1.4

- aesthetic functions.

These functions have always been fulfilled by clothing, even when people used animal skins or plant leaves to cover their body. With the development of civilization, people's needs have developed, and the possibilities of satisfying them have developed too. Today, in addition to the basic functions listed above, clothing can also play other roles. For example, it should be mentioned here a possibility of monitoring the vital functions of human body thanks to incorporation of electronic elements into clothing. Such clothing is called textronic clothing [3, 4]. Clothing can also serve as a therapeutic tool. These functions consist in supporting therapy or preventing many diseases or health problems. This group of clothing includes for instance the compression clothing or weighted clothing. Compression garments are used in lymphedema therapy to stabilize the effects of the medical treatment [5, 6]. Weighted garments provide consistent, gentle and controlled pressure to the specific areas of the body. The even and gradual compression of tissues by compression garments improves blood and lymph circulation and reduces swelling that occurs during long-term or intense exercise. Weighted clothing is used for example by athletes, but primarily by children with health problems such as: Autism, PDD (Pervasive Development Disorder), ADD (Attention Deficit Disorder), ADHD (Attention Deficit Hyperactivity Disorder), CP (Cerebral Palsy), MD (Muscular Dystrophy) and various sensory integration needs [7, 8]. However, not all children's health issues and challenges are taken into account when designing clothing. Additionally, there are many diseases that require the use of specialist medical or rehabilitation equipment for children. It should be mentioned here: spasticity, hypotonia or problems with natural nutrition.

Spasticity according to Lance's definition is "a movement disorder characterized by an increase in tonic stretch reflexes (muscle tension) in relation to the speed of stretching, which results from a disinhibited stretch reflex as a component of higher-level motor neuron damage" [9]. Spasticity can be defined as a sensory-muscular disorder that occurs as a result of upper motor neuron damage. This disorder manifests itself as involuntary, interrupted, or constant muscle activity.

Muscle laxity (hypotonia) means that the muscles tend to offer less resistance during passive joint movements. When someone moves or manipulates the limbs of a person with muscle laxity, these muscles are less resistant and more flexible, which can affect the ease of performing individual movements. Proper muscle tone is the result of the cooperation of the structures of the central nervous system with the peripheral nervous system, which leads to maintaining the fluidity of movement and maintaining the stability of the body. Muscle laxity can be caused by brain dysfunction, damage to the anterior horns of the spinal cord, problems with the peripheral nerves, disorders occurring in the neuromuscular junction and in the muscles.

There are also many diseases that require parenteral nutrition. We cannot speak here of one disease, but of several diseases, for example, problems with the oral cavity, esophagus or stomach, problems with swallowing that pose a risk of choking and food entering the lungs, or difficulty in eating enough food to meet the body's nutritional needs. Nutritional therapy is a medical procedure aimed at maintaining or improving the nutrition of people who are unable to meet the needs of the body using natural nutritional methods. Within this treatment, we can distinguish two main types of nutrition:

- enteral, which takes place through the digestive tract,
- parenteral, which involves delivering nutrients directly to the body which involves introducing nutrients directly into the bloodstream, e.g. by injection [10].

Enteral nutrition is mainly based on the use of a precisely selected industrial diet, containing all the necessary nutrients, such as protein, carbohydrates, electrolytes, vitamins, and minerals. An artificially established access to the digestive tract is used to administer food. To introduce food into the stomach, the continuous infusion method can be used, which involves gravity guidance, where the food is placed above the person and then moves using gravity. A nutritional pump can also be used. Percutaneous Endoscopic Gastrostomy (PEG) allows permanent access to the stomach. It is an easy, safe, and minimally invasive way to obtain access to food in the stomach. It is one of the most commonly performed endoscopic procedures concerning the gastrointestinal tract [11].

A tracheostomy is another health problem that may require the use of special clothing. It is a life-saving surgical procedure that involves creating an artificial airway by cutting the trachea and inserting a tracheotomy tube into its lumen in order to bypass the nose, mouth, and upper respiratory tract [12]. The most common indications for tracheostomy in children are acquired post-intubation laryngeal stenosis, congenital laryngeal and tracheal defects, prolonged intubation. The presence of tracheostomy tube may cause problems when putting on and taking off clothes. Both the mentioned above medical treatments: nutritional therapy and tracheostomy and the medical equipment used in them make it difficult for children with disabilities and their parents or caregivers to function. Currently, the market offers a very limited range of clothing for disabled children. Especially for kids lying down, the comfort of using clothing is a very important factor influencing their quality of life. The clothing available on the market often causes problems when dressing disabled children, because it is not adapted to the needs of these users. Children's clothing available on the market often has fasteners on the back or fancy frills, which can be a problem for lying children, because they cut into the body and thus cause discomfort or even pain. Another problem for disabled kids, and disable people is too tight clothing covering the lower part of the body. This is often due to the lack of movement, which causes disruption of the flow of body fluids. It can lead to swelling of the lower parts of the body. In order to ensure the well-being of disabled people and prevent discomfort, it is necessary to provide appropriate looseness in clothing, larger than in standard clothing. It can be done by appropriate pattern making and selection of appropriate materials in manufacturing the clothing for sick or disabled children. First of all, the needs of these children and their caregivers must be identified in terms of clothing that will ensure their comfort and well-being.

In the frame of presented work the survey was conducted to identify the needs of children with disabilities in the field of specialist clothing. The research was conducted among parents and caregivers of children with disabilities. Based on the survey results, some conclusions were drawn which can help to design the clothing for children with disabilities.

2. Methods

The survey was addressed to parents and caregivers of disabled children aged 1 to 18, dependent on performing basic daily activities or requiring significant assistance from parents, e.g. problems with dressing, washing, eating meals, etc. The survey was conducted using a Google Forms survey form. The link to the survey was shared on the Facebook platform in three groups: "Tracheostomy in children", "Respiratory THERAPY – home ventilation of the patient", "Parents of disabled children – discussion on any topic". Totally, 55 parents of disabled children took part in the survey. The parents of the children answered eight questions. Five of questions were closed-ended. These were the following questions:

Question No. 1. Age of the child – choice from 1 to 18.

Question No. 2. Gender of the child:

- Boy
- Girl

Question No. 3. Type of muscle tension. Is the child:

- Spastic
- Flaccid
- Spastic-flaccid

Question No. 4. Does the child have:

- PEG
- Orthosis

- Stoma
- Tracheostomy
- Other: (specify what)

Question No. 5. Is there a need for specialist clothing:

- Yes
- No
- I have no opinion.

The remaining three survey questions were open-ended:

Question No. 6. What difficulties occur when dressing the child?

Question No. 7. What solutions are missing in clothing that would make the dressing process easier and improve comfort of use?

Question No. 8. Do you use clothing designed for children with disabilities? If so, what kind (please specify the type (pants, blouse, etc.) /brand/ manufacturer).

3. Results and Discussion

The survey results are presented and discussed below. The answers to the closed questions are presented in the graphs (Fig. 1 – 5). The analysis of the survey results showed that the largest group – 38 % of all respondents – consists of children in the group I, i.e. children aged above 2 to 6 years. In this group the most often are children aged 3 years. The next largest group is the age group II, i.e. children aged above 6 to 11 years which constitutes 25 %, followed by the group IV – children aged above 15 to 18 years (16 % of all respondents), 11 % of respondents belong to the age group III, (above 11 to 15 years) while the age group 0 (babies from 0 to 2) constitutes 9 % of respondents (Fig. 1).

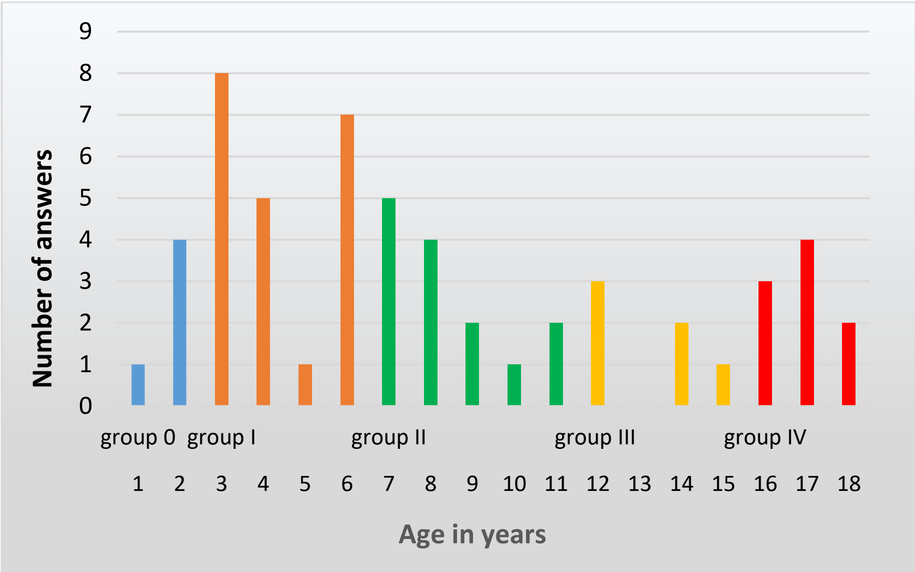

Fig. 1. Answers to the question about the child's age

Among 55 surveys collected the majority – 33 responses (66.7 %) were completed by parents of boys, while 22 responses (33.3%) were completed by parents of girls (Fig. 2).

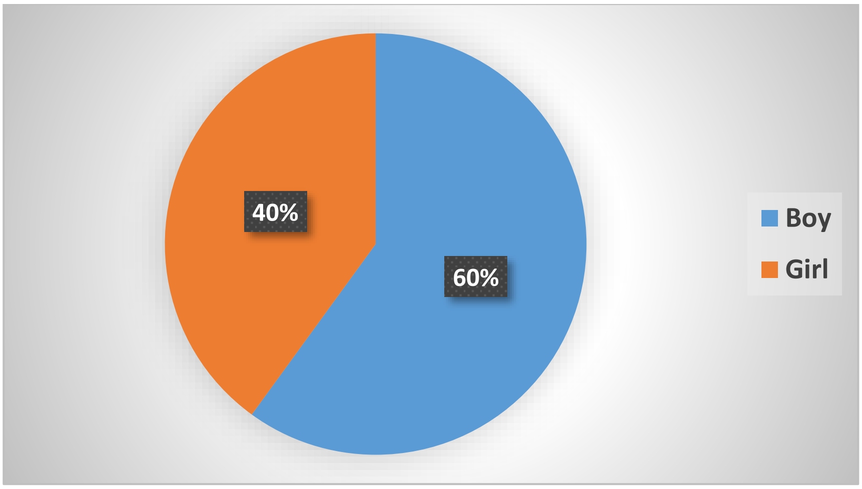

Fig. 2. Answers to the question about the child's gender

The survey showed that the largest number of parents of children with flaccidity took part in the study (55 % of all responses). Parents of children with spasticity constituted 40% of the survey participants, while parents of spastic-flaccid children constituted only 5 % of the analysed group (Fig. 3).

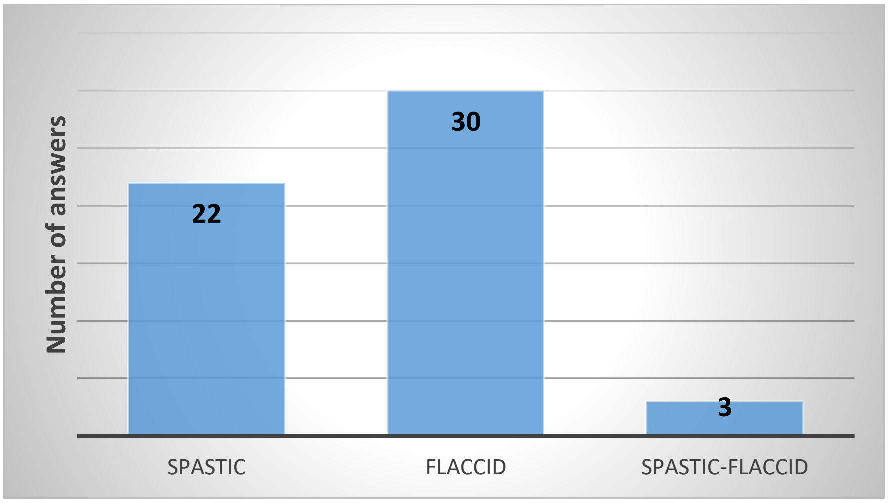

Fig. 3. Answers to the question about the type of muscle tension

Question no. 4 aimed to determine whether children have medical equipment that is important for their comfort of life. The survey showed that almost half of the children who took part in the study (45 % of all respondents) have a tracheostomy, 40 % of children have an orthosis and 38 % of children have PEG (Fig. 4). It was also stated that often, a child uses not only one medical equipment but has some type of combination, most often it is the PEG and the tracheostomy or the PEG, orthosis, and tracheostomy.

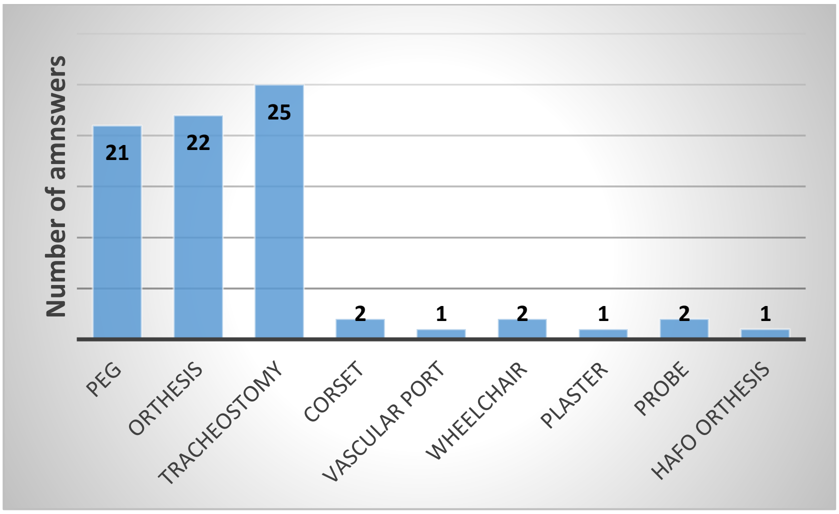

Fig. 4. Answers to the question about medical equipment owned/used by children.

The last closed question – question no. 5 concerned the demand for specialist clothing for children with health problems. The answers to this question (Fig. 5) showed that there is a demand for clothing with special purposes functionality and facilities. As many as 89 % of people who took part in the study answered that there is a demand for clothing intended for children who experience inconveniences when using clothing. Only 6 % of respondents answered that they do not see a need for clothing for people with disabilities and next 5 % of people answered that they have no opinion on the subject.

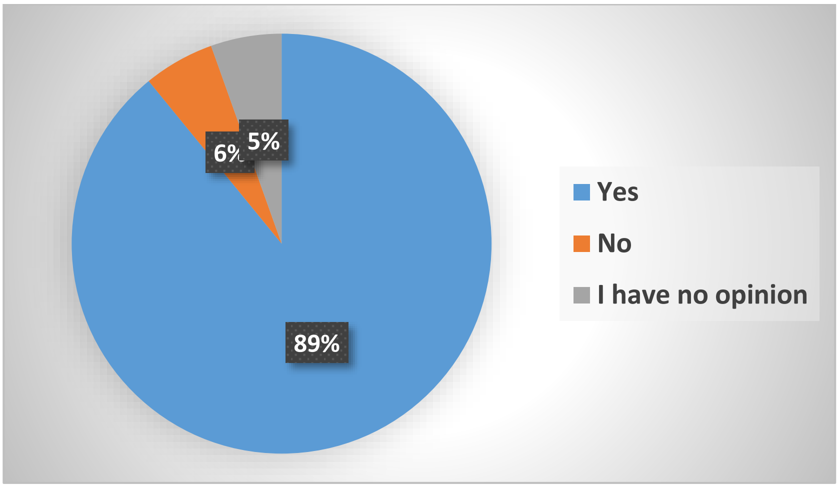

Fig. 5. Answers to the question about the specialist clothing for children with health problems

The Questions 6 – 8 are the open-ended type.

Question no. 6 concerned the difficulties occurring while dressing a child. Parents indicated the following difficulties and problems when dressing a child:

General problems:

- Synthetic materials used in clothing cause the child to sweat intensively. This can lead to an increased risk of the child getting sick, e.g. pneumonia.
- The need to turn and lift the child while dressing.
- Difficulty in putting hands into unbuttoned clothes, too little material on the back to pull on a jacket or sweatshirt when one hand is already in the other sleeve.
- Flabby arms make it difficult to put hands into sleeves, which can lead to injuries.
- Problems with putting on sweatshirts, sweaters, jackets due to wrist laxity and elbow joint contracture.
- Problems with bending the arms and lifting them up, which contributes to problems with putting on unbuttoned clothes.
- The upper part of the clothing pulls up during usage.
- Problems with putting on sweatshirts and jackets due to sleeves that are too tight.
- Spasticity makes it difficult to put hands in the sleeves.
- Problems with putting on pants due to popliteal and hip contractures.
- Difficulty in bending the limbs when dressing.
- Narrow trouser legs.
- No bodysuits available above size 92.
- Sensory hypersensitivity to textures and the touch of materials
- Irritation from clothing items that are close to the face.
- Low elasticity of clothes.

Problems when using a tracheostomy:

- The tracheotomy tube may become detached when putting on the upper part of the clothing.
- The tracheotomy tube interferes with the neckline.
- The tracheotomy tube falls out when dressing.
- Covering the tracheotomy tube by clothing during winter.

Problems when using the PEG:

- Lack of easy access to the PEG, the child must be undressed.
- There is a risk of tearing out or damaging the PEG.
- Clothes are not adopted for feeding with a PEG.
- The PEG is pressed by the elastic band in the pants; if the pants are worn lower, there is a high probability that they will slip off.

Problems when using the orthosis:

- Too narrow pants, which make it difficult to put on and take off when the orthoses are on the legs.
- Tights and leggings that tear quickly.
- Too narrow legs.
- The bottoms of the trouser legs do not stretch enough to go through the orthoses.

Question no 7. concerned missing solutions in clothing that would make the process of dressing easier and improve comfort of clothing usage. Parents/caregivers indicated the following solutions that would make the process of dressing and undressing a child easier:

General solutions:

- Full-length buttoned sleeves
- Snap-on shirts
- Clothes with fasteners in places other than the belly, e.g. buttoned sleeves, buttoned trouser legs.

- Garment that ensures thermal comfort without many layers of clothing.
- A bodysuit that looks like a T-shirt.
- Winter overalls for a stroller, consisting of a jacket and a warm leg bag attached to it with a zipper.
- Zippers in jackets along the entire length of the side seams from the wrists through the armpits to the ribs.
- Winter trousers that can be unbuttoned into two parts.
- Blouses that fasten at the neck.
- No labels, delicate seams.
- Bodysuits and rompers in large sizes, over 92.
- Romper-type clothing without feet to easy access to the pulse oximeter.
- Trousers adjustable at the waist.
- No buttons, snaps, or zippers on the back.
- Bodysuits buttoned on both sides.
- Wider, buttoned trouser legs.
- Trousers buttoned along the inside and outside seams.
- Leggings without tight bottom cuffs.
- Sweatshirts buttoned along the sleeves.
- Natural materials such as cotton, bamboo, merino.
- "Breathable" materials.

<u>Solutions for children with tracheostomy:</u>

- Soft, stretchy, reusable, fastened straps for the tracheostomy tube.
- A cutout for the tracheostomy tube.
- A winter bodysuit that will cover the tracheostomy tube so that the child does not freeze in the fall and winter.
- Turtlenecks that will allow air to flow freely so that breathing is easy.
- Scarves through which you can breathe.
- Clothes with a wide opening for the head.

- Scarves that make it easier to access the tracheostomy tube without completely exposing it to suck out secretions.
- Clothes with a wider neckline so that the clothing does not cover the tracheostomy tube.
- A wide fastener at the neckline to minimize the risk of the tracheostomy tube getting caught or pulled when putting on or taking off shirts.

<u>Solutions for children using PEG:</u>

- Wheeled pads for the PEG, preferably fastened so that they do not fall off and can be washed.
- Buttoned blouses with access to the PEG.
- Sweatshirts, bodysuits, T-shirts with an opening for the PEG, so that there is no need to undress the child when it is cold or in public places.

<u>Solutions for children using orthoses:</u>

- Clothing that allows easy access to the orthoses.
- Wider trouser and legging legs to accommodate the orthoses.
- Knee-length trousers with a zipper.
- Trouser legs with zippers on the sides, so that they can be put on by a lying down person with rehabilitation equipment.
- Higher waist, especially in the back.

The last question was the following: Do you use clothing designed for children with disabilities? If so, what kind (please specify the type (pants, blouse, etc.)/brand/manufacturer). The answers to the question show that 55 % of respondents do not use such clothing. There may be several reasons, e.g. price, lack of knowledge about the availability of such clothing, lack of larger sizes of bodysuits, lack of availability on the market, clothing does not always fulfil its purpose, is not tailored to the specific needs of the user. Parents who decide to buy this type of clothing constitute 45 % of respondents (Fig. 6).

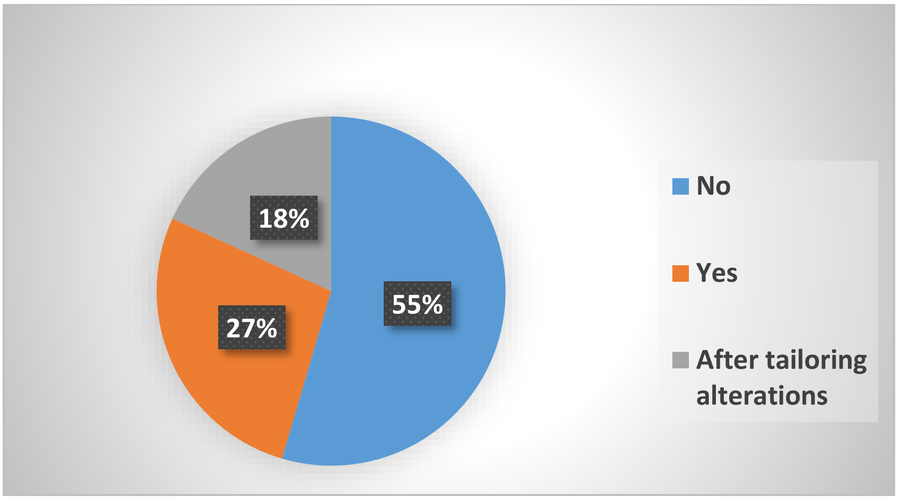

Fig. 6. Answers to the question about the clothing for children with disabilities used.

The question shows that almost half of parents who use such clothing decide to order such clothing from a seamstress or have ordinary clothes altered in such a way that they meet their needs to some extent. Most often, such clothing can be purchased online, unfortunately there are currently few companies on the market that specialize in this type of clothing. This question shows that there is a large niche in the market that has not been filled so far. We did not find any surveys in this area. The most frequently published studies concern the developmental and educational needs of children with disabilities. The presented studies are based on a relatively small group of respondents. These studies constitute a signal of the problem. The obtained results confirm that further research in this area is needed. Nevertheless, this is a niche group of recipients considering the entire population of clothing users and apparel market. Therefore, the production of such specialized clothing may be short-series, and therefore less profitable, than large-series production of standard clothing. This is the main reason why clothing adapted to the needs of children with disabilities is unavailable or available to a very limited extent.

4. Conclusions

After analysing all the responses given in the survey by parents/ caregivers of disabled children, the following can be stated:

- The biggest problem when dressing is putting hands into sleeves, both in spastic and flaccid children, because of contractures, parents have problems with manipulating their hands.
- Another proposed solution is wider trousers that can be buttoned along their entire length, which would greatly facilitate the process of putting them on.
- Most parents of children with a tracheotomy tube pointed out the high probability of the tube coming out while dressing. The neckline of blouses is also often a problem when using clothes,because it interferes with the tube or causes a risk of covering it.
- Caregivers of children with enteral nutrition indicated that ordinary clothes make it much more difficult for them to feed their children. They indicated that there is a risk of PEG tearing out and that ordinary clothes often press on the place where the PEG is located.
- In the case of children with orthoses, the biggest problem is that the clothing is too tight, which creates a problem putting on pants or shirts over the orthoses. There is also a problem when putting on clothes that do not stretch enough to be put on the orthosis.
- There are major shortages when it comes to integrated clothing for children with gastrostomy in the form of shirts/bodysuits and sweatshirts, sweaters that have an appropriate opening for the PEG in the same place.
- If there is clothing adapted to PEG on the market, it is available in the form of shirts/bodysuits, less often sweatshirts. The problem occurs when the parent wants to buy, for example, clothes such as overalls or rompers, dresses, sweaters, dungarees, or more elegant clothing in the

form of shirts.

- There are no bodysuits available above size 92.
- There is also a problem when it comes to labels because they often irritate the child's skin. If the child is sensory hypersensitive, the seams irritate their skin, as a result of which the child feels discomfort when wearing clothes.
- Parents pay a lot of attention to the materials used to make clothes. They most often choose cotton, linen and wool.
- Generally, respondents stated that the subject of the survey is very important because there is a lack of clothing that meets the needs of children with disabilities.

References

[1] Purwar S.: *Functional clothing: A review*. International Journal of Home Science, Vol. 8(1), 2022, pp. 158-161.

[2] Geršak J.: *Clothing classification systems*, in: Design of Clothing Manufacturing Processes, Woodhead Publishing Series in Textiles 2013, pp. 1-20.

[3] Leśnikowski J.: *Textile Transmission Lines in the Modern Textronic Clothes,* Fibres & Textiles in Eastern Europe, Vol. 19, No. 6 (89), 2011, pp. 89-93.

[4] Choudhry N.A., Arnold L., Rasheed A., Khan I.A., Wang L.: *Textronics – A Review of Textile-Based Wearable Electronics*, Advanced Engineering Materials, Vol. 23, 2021, 2100469

[5] Hill J., Howatson G., Van Someren K., Leeder J. Pedlar Ch.: *Compression garments and recovery from exercise-induced muscle damage: a meta-analysis*, British Journal of Sports Medicine, 48 (8), 2013, DOI: 10.1136/bjsports-2013-092456

[6] Sainia N., Yadava S.: *Applications of Compression Garments,* Just Agriculture, Vol. 3 Issue 2, 2022, pp. 1-8

[7] VandenBerg N.L.: *The Use of a Weighted Vest To Increase On-Task Behavior in Children With Attention Difficulties*, American Journal of Occupational Therapy · November 2001, pp. 621-628

[8] Buckle F., Franzsen D., Bester J.: *The effect of the wearing of weighted vests on the sensory behaviour of learners diagnosed with attention deficit hyperactivity disorder within a school context,* South African Journal of Occupational Therapy, Vol. 41, No. 3, 2011, pp. 36-42.

[9] Olchowik, B., Sobaniec, W., Sołowiej, E. i Sobaniec, P.: *Child Neurology,* Aspekty

kliniczne zwalczania spastyczności, Vol. 18, 2009, p. 49.
[10] Komasińska P. Steinborn B.: *Dziecko wiotkie z punktu widzenia pediatry i neurologa dziecięcego*, Child Neurology, Vol. 29/2020, nr 59, 2020, pp. 27-28.
[11] Bartoszewska, L. Majewska, K. Matras, P.: *Żywienie dojelitowe i pozajelitowe*. Wydanie I, Wydawnictwo Naukowe PWN S.A., Warszawa 2023.
[12] Rudzki, B., Żwirełło, A., Burdyn G., Kaźmierczak-Siedlecka K., Lubieniecka-Archutowska E. i Lebiedzińska A.: *Żywienie enteralne pacjentów pediatrycznych z rozpoznaną chorobą Leśniowskiego-Crohna*, Farmacja Polska Tom 76 nr 3, 2020, pp. 172-173.

The impact of packaging on the microbiological quality of breakfast cereals

Katarzyna Śliżewska*, Agata Nowakowska, Tomasz Piotr Olejnik, Elżbieta Sobiecka

Lodz University of Technology, Faculty of Biotechnology and Food Sciences, Lodz, Poland

Abstract

The aim of the paperwork was to study the microflora found in breakfast cereals available in stores, and to assess the effect of packaging on the microbiological product quality. The flakes tested were hermetically packed and sold by weight. The microbiological analysis included determination of the total number of mesophilic microorganisms, the total number of aerobic bacteria and mould, coagulase-positive bacteria of the *Enterobacteriaceae* family, including coliform bacteria, *Salmonella*, and *Shigella*. It was found that spore bacterial and moulds of the *Aspergillus* and *Penicillum* genus were the dominant microflora that contaminated flakes. There were no coagulase-positive staphylococci and *Salmonella* and *Shigella* bacteria. The most contaminated products were cocoa balls and wheat flakes with rice sold by weight. In general, lower contamination levels were found in hermetically packaged flakes than in those sold by weight.

Keywords: breakfast cereals, microbial contamination.

1. Introduction

The basis of human nutrition according to the food pyramid should be whole grain products, rich in health-promoting ingredients such as dietary fiber, minerals and vitamins. Numerous nutritional studies confirm that regular consumption of whole grain products has a beneficial effect on the human body, reducing the risk

* corresponding author e-mail: katarzyna.slizewska@p.lodz.pl
DOI: 10.57636/69.2024.1.5

of many lifestyle diseases, including obesity, cardiovascular diseases, diabetes and cancer [1].

Due to the increasing nutritional awareness of consumers and the search for products with high nutritional value, cereal flakes are still popular among consumers [2]. The products are aimed at a wide range of recipients, from preschool children to the elderly. A definite advantage of breakfast cereals is the variety of choices and the possibility of consuming them without additional heat treatment. The most popular breakfast cereals chosen by consumers are: oat flakes, corn flakes, flavored cereal flakes (chocolate, cinnamon, honey, etc.), muesli mixes, or granola [3].

Cereal grains, the product from which cereals are made, are an agricultural raw material particularly susceptible to contamination at every stage of production, from cultivation to processing. Microbiological contamination is one of the most serious threats associated with cereal grains and can occur at many stages of the food supply chain, such as cultivation, harvest, transport, storage, preparation and handling. These contaminants can reach cereal grains already in field conditions, transferred by various biotic (e.g. wild animals and insects) and abiotic (e.g. air, dust, water and equipment) factors present in the supply chain [4]. The number of microorganisms present in the grain and their species diversity depend on many factors, such as the location of cultivation, climatic conditions and the type of grain. Cereals growing in both cool and warm and humid climates are susceptible to contamination. In addition, grain is often subject to secondary infection during storage [5]. The microflora inhabiting cereal grains is divided into surface (epiphytic) and subsurface microflora. Surface microbiota includes bacteria, fungi and yeasts. Subsurface microflora develops mainly during grain storage, which leads to its spoilage [6].

The aim of the study was to assess the microbiological status of breakfast cereals available on the market and to determine the impact of packaging on the microbiological quality of these products.

2. Materials and methods

The study involved 8 breakfast cereals available for sale in hermetic packaging and by weight (tab. 1).

Tab. 1. Breakfast cereals tested (own study based on the data on the packaging).

Product	Packaging form	Composition
Cornflakes	foil packaging	Corn grits, sugar, salt, invert sugar syrup, molasses, enriching substances: vitamins (B3, B5, B2, B6, B9)
	by weight	Cornmeal 94%, sugar, salt, vitamin premix with iron: B vitamins, vitamin E, iron, salt
Cocoa balls	foil packaging	Whole grain wheat flour 53.1%, sugar, corn flour 17.2%, glucose syrup, low-fat cocoa 5.6%, enriching agent (mineral: calcium), contains sunflower and/or palm oil, salt, enriching agents (mineral: iron; vitamins: B3, B5, B2, B6, B1, B9, D)
	by weight	Flour 51% (whole wheat, rice, cornmeal), sugar, cocoa powder 4.9%, sunflower oil, salt, vitamin premix with iron: vitamin B1, vitamin B2, vitamin B6, vitamin B12, niacin (vitamin B3), folic acid (vitaminj B9), pantothenic acid (vitamin B5), vitamin E, iron
Muesli	foil packaging	Whole grain wheat 41.7%, rice 17%, raisins 15.9%, wholegrain oats 6.6%, sugar 5.1%, candied pineapple pieces 4.6% (pineapple, sugar, acidity regulator (citric acid), candied papaya pieces 1.9% (papaya, sugar), coconut chips pieces 1.8%, barley malt extract, sweetened dried cranberry pieces 1% (cranberries, sugar, rice flour, sunflower oil), glucose syrup, oat fiber, dried apple pieces 0.5%, salt, oligofructose, emulsifier, antioxidant
	paper tube	Cereal flakes 45% (wheat, oat), roasted peanuts 11%, walnuts 9%, dried dates 9% (dates 95%, rice flour), raisins (raisins, sunflower oil), dark chocolate 5.5% (cocoa mass, sugar, cocoa butter), spanish sage seeds /chia 5.5%, expanded wheat with honey (expanded wheat grains, honey)
Oat flakes	paper packaging by weight	Gluten-free whole grain oat flakes 100% Oat flakes 100%
Wheat flakes with rice	foil packaging	Whole grain wheat 50.9%, rice 37.3%, sugar, wholegrain oat flakes 7.1%, invert sugar syrup, barley malt extract (barley, malted barley), enriching agent (mineral: calcium), salt, glucose syrup, molasses, antioxidant (mixture of tocopherols), enriching agents (mineral: iron; vitamins: B3, B5, B2, B6, B9)
	by weight	Whole wheat flour 80%, sugar, rice 5%, salt, baking powder (raising agent: sodium carbonates, wheat flour, acidity regulator: diphosphates), wheat gluten, barley malt extract

Granola	paper tube	Granola 91.5% (oat flakes, wheat flakes, date syrup, chicory root fiber, rice flour, sunflower seeds, low-fat cocoa), dark chocolate 5% (cocoa mass, sugar, cocoa butter, emulsifier), freeze-dried raspberries 3.5%
Cocoa shells	foil packaging	Whole grain wheat flour 35.1%, chocolate powder 22.5% (sugar, cocoa 7.2%, wheat flour 17%, corn flour 15.3%, glucose syrup, sugar, barley malt extract, sunflower oil, enriching substance (mineral: calcium), emulsifier (lecithins), salt, enriching substances (mineral: iron; vitamins: B3, B5, B2, B6, B1, D
	by weight	Wheat flour 64.1%, sugar, low-fat cocoa 3.6%, cocoa 2.6%, glucose syrup, vegetable fat (palm), salt, emulsifier

The microbiological analysis of dried fruit included the definition of:

- the total number of mesophilic microorganisms (on PCA medium),
- the total number of oxygen sparing bacteria (on the PCA medium after subjecting the sample to the so-called thermal shock),
- microorganisms of the *Enterobacteriaceae* family (on the VRBG medium),
- coliforms and β-glucuronidase positive *Escherichia coli* (on the Chromocult®TBX medium),
- *Salmonella* and *Shigella* bacteria (on the SS medium),
- number of coagulase-positive staphylococci (on the Baird-Parker's medium),
- number of filamentous fungi (on the Sabouraud substrate).

10-fold dilutions of the analyzed samples were prepared and then cultured on Petri plates. Microbiological tests were conducted using the culture method in accordance with PN-EN ISO standards [7-10].

The identification of filamentous fungi was based on macroscopic observations of growth observations in plate cultures and based on microscopic observations.

3. Results and discussion

Based on the obtained results (tab. 2), a diverse number of bacteria, both mesophilic and sporulating were found in the analyzed breakfast cereals. Based on the obtained results (tab. 2), a diverse number of bacteria, both mesophilic and sporulating were found in the analyzed breakfast cereals. The presence of mesophilic bacteria was not detected in packaged breakfast cereals (corn flakes, oat flakes, wheat flakes with rice), and if they did occur, they were in small quantities, around 2 Log_{10}CFU/g. In cereals sold by weight, the number of mesophilic bacteria was higher and ranged from 3 to 5 Log_{10}CFU/g.

Aerobic sporulating bacteria were not present in corn and oat flakes in either hermetic packages or sold by weight, and in cocoa balls and wheat flakes with rice in foil packages. In the remaining breakfast cereals, the number of aerobic sporulating bacteria was not high and ranged from 1 to 2 Log_{10}CFU/g.

Cereal grains are often contaminated with mesophilic microorganisms. The primary contamination of grain can easily multiply due to inadequate raw material storage and improper technological processing. Because the conditions of the drying process are unfavorable for microorganisms (high temperature maintained for a long time), most vegetative forms, especially during logarithmic growth, are lost. However, the process parameters can be withstood by microorganisms that have developed defense mechanisms that make them resistant to high temperatures. An example is bacterial spores, whose high heat resistivity results from their structure and chemical composition. While vegetative cells die after 10 minutes of heating at 80°C, endospores can withstand even hours of heating. In their structure they contain up to 15% water and dipicolinic acid the complexes with calcium ions of which allow them to survive the drying process [11].

The limits for the number of bacteria in breakfast cereals are set by national and EU regulations on microbiological criteria for food. In the European Union, including Poland, these regulations are included in Commission Regulation (EC) No. 2073/2005 on microbiological criteria for foodstuffs. Although this regulation does not specify specific limits for breakfast cereals, they can be classified as ready-to-eat products.

The total number of mesophilic bacteria can be used as an indicator of the overall hygienic quality of the product. However, the values may vary depending on the specifications set by food manufacturers. The content of the total number of mesophilic bacteria in cereal products should be in the range of 10^3 to 10^6 CFU/g, according to the above Regulation. The obtained results of the number of bacteria were much lower, which means that they were within the norm.

Tab. 2. Total number of mesophilic and sporulating microorganisms.

Product		**Number of microorganisms [Log_{10}CFU/g]**	
		mesophilic	**sporulating**
Cornflakes	packaging	Ab	Ab
	by weight	3.15 ± 0.2	Ab
Cocoa balls	packaged	2.30 ± 0.1	Ab
	by weight	5.15 ± 0.4	1.08 ± 0.2
Muesli	packaged	2.91 ± 0.1	2.78 ± 0.1
	packaged	2.30 ± 0.3	1.76 ± 0.3
Oat flakes	packaged	Ab	Ab
	by weight	3.60 ± 0.3	Ab
Wheat flakes with rice	packaged	Ab	Ab
	by weight	5.04 ± 0.1	2.00 ± 0.2
Granola	packaged	2.08 ± 0.1	1.08 ± 0.1
Cocoa shells	packaged	2.06 ± 0.2	1.01 ± 0.1
	by weight	1.30 ± 0.1	1.12 ± 0.1

Ab – absent in 10 g; ± SD (Standard Deviation)

The presence of *Enterobacteriacea* bacteria was noted only in corn flakes by weight and oat flakes by weight. Their numbers were low and ranged from 0.4 to 0.7 Log_{10}CFU/g. In the remaining products, no *Enterobacteriacea* bacteria were found in 10 g. No coliform bacteria were found in any of the breakfast cereals analysed (tab. 3).

The main source of secondary pollution of dried fruits is man. We have a rich microflora on our skin and in the digestive tract. It was man who could be the reason for the presence of bacteria from the *Enterobacteriaceae* family in the analysed products.

Tab. 3. The number of microorganisms from the *Enterobacteriaceae* family and from the *coli* group

Product		**Number of microorganisms [Log_{10}CFU/g]**	
		mesophilic	**sporulating**
Cornflakes	packaging	Ab	Ab
	by weight	0.7 ± 0.1	Ab
Cocoa balls	packaged	Ab	Ab
	by weight	Ab	Ab
Muesli	packaged	Ab	Ab
	packaged	Ab	Ab
Oat flakes	packaged	Ab	Ab
	by weight	0.4 ± 0.1	Ab
Wheat flakes with rice	packaged	Ab	Ab
	by weight	Ab	Ab
Granola	packaged	Ab	Ab
Cocoa shells	packaged	Ab	Ab
	by weight	Ab	Ab

Ab – absent in 10 g; ± SD (Standard Deviation)

None of the tested products sold both in hermetically sealed containers and by weight, were contaminated with *Salmonella* and *Shigella* bacteria and coagulase-positive staphylococci.

The presence of filamentous fungi was found in the following flakes: corn flakes by weight, cocoa balls by weight, muesli in foil and paper packaging, oat flakes by weight, wheat flakes with rice by weight (tab. 4). The number of filamentous fungi in the flakes varied, ranging from 1.00 to 4.90 Log_{10}CFU/g. The highest content of filamentous fungi was found in the sample of muesli flakes in a foil package. The high content of mould fungi in this product could be caused by the presence of microbiologically contaminated dried fruit present in the muesli.

However, analyzing which filamentous fungi were on the breakfast cereals on macroscopic and microscopic observations, it was found they belong to the *Aspergillus* genus and the *Penicillum* genus (tab. 4, fig. 1).

Tab. 4. Number of filamentous fungi

Product		Number of mould [Log_{10}CFU/g]	Morphological identification
Cornflakes	packaging	Ab	-
	by weight	1.48 ± 0.2	*Penicillum*
Cocoa balls	packaged	Ab	-
	by weight	4.20 ± 0.1	*Aspergillus*
Muesli	packaged	4.90 ± 0.3	*Aspergillus*
	packaged	1.00 ± 0.1	*Aspergillus*
Oat flakes	packaged	Ab	-
	by weight	1.3 ± 0.2	*Aspergillus*
Wheat flakes with rice	packaged	Ab	-
	by weight	2.45 ± 0.2	*Penicillum*
Granola	packaged	Ab	-
Cocoa shells	packaged	Ab	-
	by weight	Ab	-

Ab – absent in 10 g; ± SD (Standard Deviation)

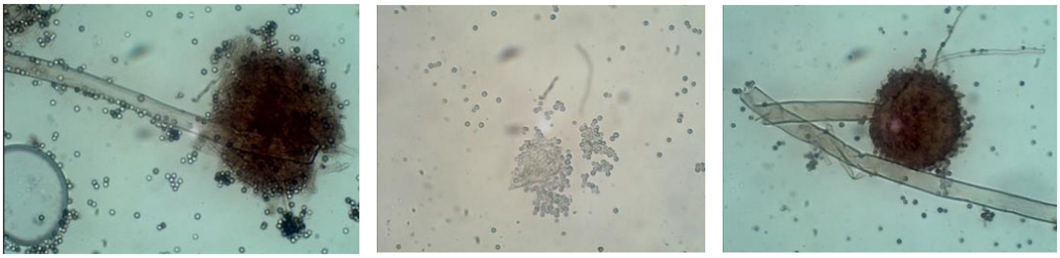

Fig. 1. Morphology of selected filamentous fungi (microscopic observations, x40).

4. Conclusion

Based on the microbiological analysis, it was found that bacterial spores and moulds of the *Aspergillus* and *Penicillum* genus were the dominant microflora that contaminated breakfast cereals. There were no coagulase-positive staphylococci and Salmonella and Shigella bacteria. The most contaminated product were cocoa balls and wheat flakes with rice sold by weight and muesli in foil packaging. In general, a low level of microbiological contamination of the studied cereals and a lower level of contamination of hermetically packaged cereals were found than in those sold by bulk.

References

[1] Sobota A., Rzedzicki Z., Sobieraj M.: *Badanie składu chemicznego płatków musli*. Bromatologia i Chemia Toksykologiczna, 45(2), 2012, pp. 131-137.

[2] Priya K.M., Sivakumar A.*: Analyzing consumer behaviour towards food and nutrition labeling: A comprehensive review*. Heliyon, 9(9), 2023, pp. 1-18.

[3] Williams P.G.: *The Benefits of Breakfast Cereal Consumption: A Systematic Review of the Evidence Base*. Advances in Nutrition, 5(5), 2014, pp. 636S-673S.

[4] Los A., Ziuzina D., Bourke P.: *Current and Future Technologies for Microbiological Decontamination of Cereal Grains*. Journal of Food Science, 83(6), 2018, pp. 1484-1493.

[5] Magan N., Aldred D. *Managing microbial spoilage in cereals and baking products*, [w:] *Food spoilage microorganisms*, C. Blackburn (red.), Woodhead Publishing Ltd, Cambridge, UK, 2006, pp. 194-212.

[6] Nierop S.V. *The impact of microorganisms on barley and malt quality - A review*. Journal of the American Society of Brewing Chemists, 64(2), 2006, pp. 69-78.

[7] PN-ISO 21527-2:2009. Food and feed microbiology. Horizontal method for the enumeration of yeasts and molds.

[8] PN-ISO 21528-2:2005. Food and feed microbiology. Horizontal method for the detection and enumeration of *Enterobacteriaceae*.

[9] PN-ISO 4833:2004. Food and feed microbiology. General rules for the determination of the number of microorganisms.

[10] PN-ISO 6888-1:2001/A1:2004. Food and feed microbiology. Horizontal method for the determination of the number of coagulase-positive staphylococci (*Staphylococcus aureus* and other species).

[11] Kołożyn-Krajewska D.: *Microorganisms in food - risks or benefits*. Żywności. Nauka. Technologia. Jakość, 3(4), 1995, pp. 21-31.

The dynamic behavior of the multi-frequency vibrating screening

Krzysztof Siczek [1], Marek Woźniak [1], Maciej Kuchar [1], Adam Rylski [2], Remigiusz Modrzewski [3], Andrzej Obraniak [3], Katarzyna Ławińska [4,*] , Malwina Wachulak [5], Radosław Świątecki [6]

[1] Department of Vehicles and Fundamentals of Machine Design, Lodz University of Technology, Lodz, Poland

[2] Institute of Materials Science and Engineering, Lodz University of Technology, Lodz, Poland

[3] Faculty of Process and Environmental Engineering, Lodz University of Technology, Lodz, Poland

[4] Łukasiewicz Research Network – Lodz Institute of Technology, Lodz, Poland

[5] GoudenKorrel S.A, Kaliska, Poland

[6] Spoldzielnia Inwalidow ZGODA, Konstantynow Lodzki, Poland

---

Abstract

The article aimed to compare the results of the experimental and the simulation research on the dynamic behaviour of the developed multi-frequency vibrating screen prototype. A simulation model of the screen and a test stand for trajectory research have been developed. Simulations of the screen motion were carried out and the results obtained from measurements on the test stand were compared. It was noticed that for the angular ratio of the rotational speeds equal to 1 under their reverse synchronization for the two rotary vibrators exciting the analyzed screen the best conditions were obtained for the good segregation of the granular layer on the screen.

Keywords: screen; dynamics; multi-frequency vibrator; grain

---

1. Introduction

Nowadays, vibrating screens, conveyors, rammers, and machines for processing loose materials are mainly used in mining, metallurgy, construction, etc. [1]. It is

[*] corresponding author e-mail: katarzyna.lawinska@lit.lukasiewicz.gov.pl
DOI: 10.57636/69.2024.1.6

known that the shape of the trajectory of the screen during its operation affects the achievement of the best processing properties of the machine. In the case of vibrating screens used for coal processing, the motion of the screen may be a circular, elliptical, or straight line. Linear is used in horizontal, high-frequency and banana screens. Elliptical can also be used on horizontal and banana screens [2]. The banana screen uses a curved banana-shaped deck instead of a flat deck equipped with a horizontal screen [2]. It has been found that elliptical motion provides greater efficiency compared to machines with linear and circular motion [3]. More complicated, complex sieve movement affects the ability to segregate grains in that it causes better mixing of the grain layer on the sieve, which allows smaller grains to reach the sieve surface and be separated. The main sieving resistance is in the layer of material on the sieve and the movement of the sieve and this layer is crucial for the efficiency and effectiveness of sieving. Basalt aggregate with a grain size of 0.1 - 2.0 mm was used as a model material for screening in later screening process studies (not included in this article). This material is difficult to screen due to its sharp-edged grain shapes and high internal friction coefficients. The screening efficiencies obtained for multi-frequency drives were in most cases higher by 5 - 10% compared to the single-frequency drive. The trajectories of the vibratory movement lead to intensive grain segregation layers moving on the sieve. Simonyan and Yiljep [4] developed a grain threshing machine and conducted studies of grain separation and the distribution of the cleaning efficiency of the cleaning unit, fractionated by sieve and horizontal airflow along the entire length of the sieve. They studied the influence of feed rate, air velocity and sieve oscillation frequency on cleaning efficiency. The research confirmed that the cleaning efficiency decreased with the increase of the sieve oscillation frequency and the feed rate of the raw material. At the same time, as this frequency increased, cleaning loss, feed rate, and air velocity increased. Aipov noticed [5] that the more complicated the kinematics of the oscillating sieves, the more it affects the screening efficiency. The deterioration of the screening process is associated with the wear and ageing of their mechanical components [6, 7]. The drive of the vibrating machines presented in [8, 9, 10] was based on a rotary to-reciprocating converter. Complicated the kinematic scheme of the presented drive increased the cost of the machine, while at the same time impairing energy efficiency and energy reliability due to many rubbing and wearing surfaces. Yarullin et al. [11] introduced a vibrator with adjustable frequency using counterweights. It proposes regulation at the expense of even more complex kinematics, i.e., the use of complementary kinematics spring counterweights. Linenko et al. [12] described a complex oscillation using the normal plane force linear asynchronous motor (LAM). They developed an adaptive LAM control system that allows the stabilization of vibration parameters. LAM allowed direct movement of the working body and an energy-saving electric vibrating drive. LAM and other electric drives can force reciprocating motion. As mentioned in [13], linear electromagnetic transducers are mainly used to generate vibrations. The authors determined a mathematical model of the electromechanical structure with the inverse circular motion of bodies connected by spring bonds and stimulated by a drive coil. According to [5] regulated linear induction motors (LIN) are used in traction machines for transport during magnetic levitation. In electric drives using the reciprocating movement of working parts in the range of sieve vibration frequency grain cleaning machines, continuous change of secondary element resistance is not recommended as it leads to increased wear rubbing elements and increased resistance to movement. The screening process is related to the purification of some of the remaining ingredients from the previous process, for example, core granules with successive functional layers. The intensity of grain mixing remains on and the sieve and its proper selection of intensity to the required properties of the final product are of particular importance for the final screening product. The mass of material remaining on the vibrating sieve undergoes intensive mixing. Two can be mentioned sources of influence that positively influence this complex process. Grains of sifted material lying on the sieve are subject to the force of gravity, friction, and elasticity effects of the sieve or its frame, and the forces of inertia. During the vertical oscillations of the sieve, for every single grain in the sieve, its potential energy is converted into kinetic energy and vice versa. At this time, the effects of friction and deformation of adjacent grains they can cause time-delayed linear and rotational displacements relative to the screen. This movement of the grains promotes the mixing of the mass material remaining on the screen. There may also be delays in grain displacement with horizontal oscillations of the screen. Friction forces from the surface of the screen and deformation forces from the frame acting on the grains adjacent to them have the main effect on the displacements. These interactions are transferred to subsequent grains due to friction and deformation between them. As a result, additional, time-delayed resultant linear and rotational displacements of grains are created. Friction forces depend mainly on non-linear changes in grain velocity when performing relative grain displacements, and to a lesser extent from moving grains associated with changes in the value of the friction coefficient. The inertial forces are directly proportional to the changes in the velocity of the grains. Therefore, the mixing intensity of the screened material is proportional to the intensity of the change in the screening speed.

One of the problems affecting the efficiency of screening is the clogging of the sieves. The more intensive movement ensures easier self-cleaning of the sieve. In addition, it was shown by Lawinska and Modrzewski [14] that for higher vibration frequencies and amplitudes, machines with vibrating screens had a lower tendency to clog the screen openings. Li et al. [15, 16] showed that increasing the vibration intensity increased the efficiency of screening materials, but at the same time increased the loss of materials during selection. While studying the accuracy of vibrating screening of materials with different properties (size and shape), Elskamp and Harald [17, 18] found that the horizontal particle velocity component was stronger than the vertical one. This ensured greater screening accuracy. Yan [19] described that the best screening accuracy in linear vibrators could be obtained for the excitation frequency in the range from 18 Hz to 20 Hz, and particle flow below

0.4 kg/s. Vibrating screens are characterized by the spatial, non-linear vibrating motion of their sieves. They have six degrees of freedom and can vibrate longitudinally in all three directions in space and torsionally about three mutually perpendicular axes. This is due to the drive system, which is designed to provide stimulating forces in selected directions, and the suspension system having susceptibility to elastic deformation for six degrees of freedom. The screens are driven by at least two independent drive vibrators, not mechanically synchronized by gears. This allows different stimulation frequencies to be used forces in individual drive units. For screening fine wet particles or small aperture particles Peng et al. [20] described a cantilever vibrating screen (CVS) with open screen holes, composed of cantilever sieve bars. This construction was characterized by a high probability of breaking through the sieve, rather than through the traditional sieves. The authors reported that additional vibrations appeared during the body of the screen movement and a smaller difference between the natural circular frequency and the vibration frequency can result in higher vibration amplitude of the screen. Multi-frequency vibrating screens can be used for sorting and additional (relatively effective) drying of products on the sieve, formed in the torrefaction process [21-23]. Li and Chen [24] reported that the granular block material can be quickly loosed and fully layered when entering the vibrating screen if an exciting system with low frequency and large amplitude is placed at the feeding end. The additional exciter with a high frequency and a small amplitude set near the discharging end acting on the granular material can lower the phenomenon of blocking the screen holes by such material. For the elliptical vibrating screen system, the compound nonlinear screening trajectories can be obtained from the two-times frequency vibrating synchronization system driven by three exciters. Vibrating screens often contained springs to influence their movement. Liu et al. [25] described that spring failures cause structural damage and low shielding performance of mining vibrating screens. Spring damages should be effectively diagnosed for timely maintenance to ensure the safety and reliability of screens.

To perform a complex motion of the sieve, allowing better mixing of screened material, with the possibility of adjustment at the same time the amplitude and frequency of the sieve vibrations, but without interfering with the sieve resistance secondary circuit elements of the vibrators used, prototype screen was developed belonging to the group multi-frequency screens shortly characterized in the next chapter. By choosing the right proportions of the vertical and horizontal amplitudes for the vibratory motion of the screen, it is possible to obtain an optimal course of the screening process to limit the clogging of the screen and the assumed structure of the screened material with the saved energy efficiency of the screen. To recognize the nature of the dynamic behaviour of multi-frequency screens, it is necessary to conduct simulations and/or experimental research. The prototype multi-frequency screen was developed and utilized for the experimental studies on its dynamic behaviour described in the further chapter. Also, the mathematical model of such a prototype screen was elaborated and used for the simulations of the dynamics of such a screen, as described further in the article. The article aimed to compare the results of the experimental and the simulation research on the dynamic behaviour of the developed multi-frequency vibrating screen prototype.

2. Methods

2.1. Prototype staggering and circulating screen

The experimental recoiling and revolving sifter with a replaceable unit driving the sieve frame is mounted on a universal test stand. The angle α of inclination of the screen to the horizontal was equal to 15°. The diagram of this stand with the screen is shown in Fig. 1. The screen included a discharge hopper with a gate 1, a sieve frame 2 suspended or supported on an elastic suspension, a container for the sifted through product 3, a container for the sifted out product 4, supporting structure 5. For the measurements, a steel wire woven sieve with a square hole size equal to 0.63 mm, a length of 1.2 m, and a width of 0.39 m was used. The granular material was fed to the sieve through the discharge hopper 1. Sifted through and sifted out grain masses were collected into special containers 3 and 4, respectively, placed under and near the screen and weighed in controlled periods. A characteristic feature of this sifter was the location of the extreme vibrators (2), which synchronized consistently or oppositely cause the staggering movement of the sieve frame in the sieve plane. That movement was overlaid with the circular movement caused by the central vibrator (1) placed under (Fig. 2a) or above (Fig. 2b) the cuboidal sieve frame. These vibrators were rotary ones rotating at a certain angular velocity. The conditions of dynamic synchronization of individual vibration exciters (vibrators) were important. Extreme vibrators 2 and 3 usually run at the same rotational speed (consistent and opposite rotating synchronization). The central vibrator 1 might rotate at the same or different rotation speed than the extreme vibrators 2 and 3. The same rotational speed was used in the tests. An important feature of this machine was the ability to change the drive operation and obtain a smooth, even grain layer movement on the screen.

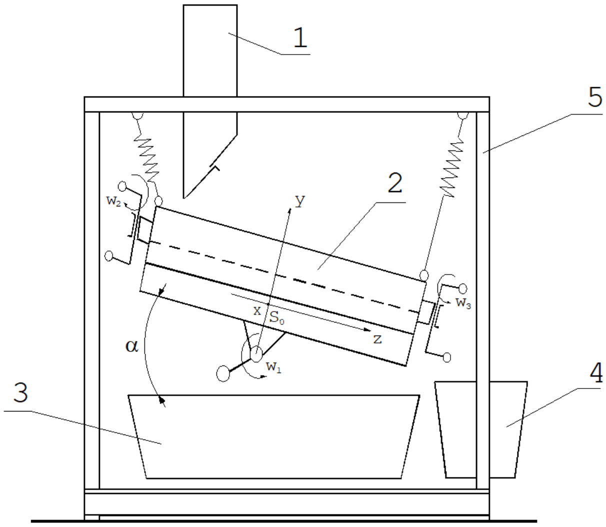

Fig. 1. Test stand with the prototype screen; 1 - discharge hopper with a gate, 2- sieve frame suspended or supported on an elastic suspension, 3 - container for the sifted-through product, 4 - container for the sifted-out product, 5 - supporting structure.

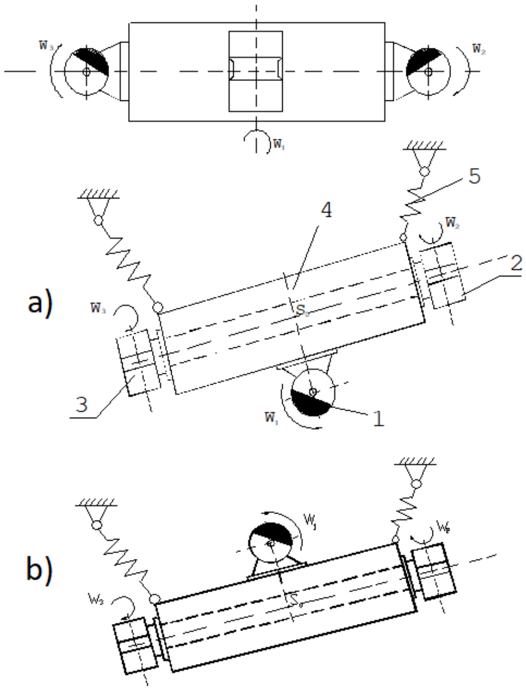

Fig. 2. Positions of vibrators on the prototype screen; 1 – central vibrator, 2- left extreme vibrator, 3 – right extreme vibrator, 4 – sieve frame, 5 – springs of supporting structure; a) configuration with the central vibrator 1 under sieve frame 4; b) configuration with the central vibrator 1 above the sieve frame 4.

There were five possible configurations of the rotational speeds of the vibrators 1, 2, and 3 (Figure 2):

1) $w_2 = w_3, w_1 = 0$ (vibrators 2 and 3 rotating in unison with vibration 1 turned off),

2) $w_2 = -w_3, w_1 = 0$ (vibrators 2 and 3 rotating in opposite directions with vibrator 1 turned off),

3) $w_2 = w_3 = w_1$ (vibrators 2 and 3 rotating in unison with vibration 1 turned on),

4) $w_2 = -w_3 = w_1$ (vibrators 2 and 3 rotating in the opposite direction with vibrator 1 turned on),

5) $w_2 = w_3 = 0, w_1 \neq 0$ (only vibrator 1 was turned on).

The vibrator 1 only rotated in one direction, in the direction of the inclination of the screen.

2.2. Measuring apparatus

The measuring apparatus, the diagram of which is shown in Figure 3, consists of the following elements: piezoelectric sensors, an integrating circuit and a computer equipped with a PCL-818 HD measurement card. The sensors, under the influence of acceleration, generate a voltage signal, which is then sent to the integrator.

Sensor parameters (sensitivity):

- acceleration: 10 mV / (m/s^2),
- speed: 10 mV / (mm/s),
- deflection: 10 mV / µm.

The voltage signal produced by the sensors is integrated twice, as a result of which we obtain the value of the riddle deflection. These signals are collected by the measurement card and saved in a digital form in computer memory.

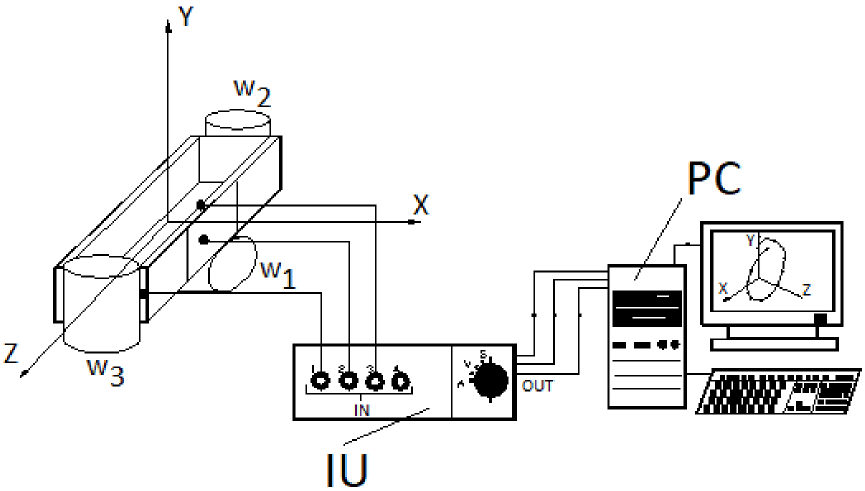

Fig. 3. Measuring apparatus; PC – personal computer, IU – integrated unit, w_1, w_2, w_3 – rotational speed of vibrators 1, 2, 3, respectively.

The measurements of sieve paths were made with the use of three sensors working on a common time base, which allowed us to determine the spatial image of vibrations. The measurement sensors were mounted on the screen in such a way that their measurement lines intersect within the centre of gravity of the screen. The mounting points of the sensors for spatial measurements are shown in Figure 4. After connecting the measuring system, measurements were made for several types of drive and variable positions of unbalanced masses on the shafts of vibrators. The results were saved on a computer disk.

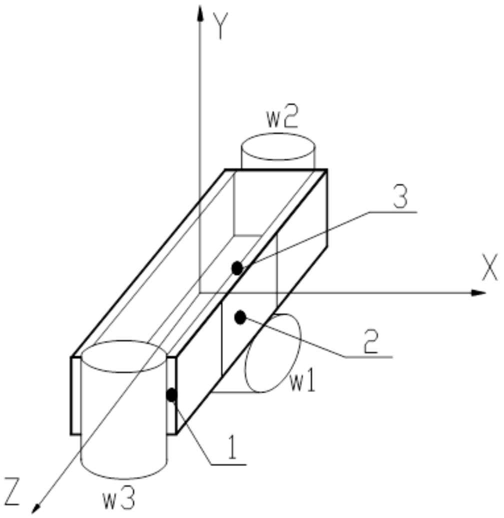

Fig. 4. The mounting points of the sensors for spatial measurements; 1, 2, 3 – sensors, w_1, w_2, w_3 – rotational speed of vibrators 1, 2, 3, respectively.

Based on the results of vibration path measurements, the maximum amplitudes were determined. Moreover, the values of the grain's throwing coefficient marked by K were determined and registered. For the case of spatial vibrations, the determination of the coefficient K is quite specific. There is no component of the gravitational acceleration g in the X direction. Thus, it was assumed that the uplift in the direction of the X axis, which does exist, has a negligible impact on the dynamics of the grain movement on the sieve. Therefore, only the rip-up in the direction of the Z and Y axes was considered (Fig. 5). The grain's throwing coefficients in these directions were determined from equations (1) and (2):

$$K_Y = \frac{a_Y}{g \cdot \cos\alpha} = \frac{A_Y \cdot \omega^2}{g \cdot \cos\alpha} = \frac{A_Y \cdot (2\pi \cdot n)^2}{g \cdot \cos\alpha}, \quad (1)$$

$$K_Z = \frac{a_Z}{g \cdot \sin\alpha} = \frac{A_Z \cdot \omega^2}{g \cdot \sin\alpha} = \frac{A_Z \cdot (2\pi \cdot n)^2}{g \cdot \sin\alpha}, \quad (2)$$

where:

α - the angle of inclination of the sieve,

n – rotational speed of vibrator [rpm],

g = 9.81 m/s^2 - gravitational acceleration,

a_Y – acceleration amplitude measured in the Y direction,

a_Z – acceleration amplitude measured in the Z direction.

The resultant grain's throwing coefficient K_R was determined from equation (3):

$$K_R = \sqrt{K_Y^2 + K_Z^2}, \quad (3)$$

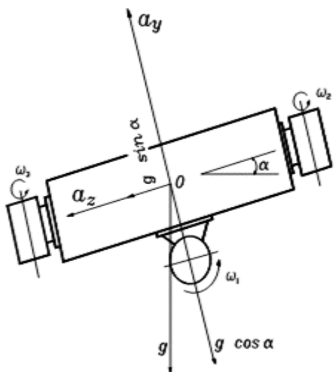

Fig. 5. The grain's throwing directions considered during measurements.

2.3. Simulations

2.3.1. The physical model of the dynamics of the staggering and circulating screen

The simulation model comprised physical model, wherein the moving sieve frame was treated as a rigid body with mass M and moments of inertia concerning the main axes I_x, I_y, and I_z. The sieve frame was suspended by a system of four identical springs with vertical stiffness k_y and transverse stiffnesses k_x and k_z. In the equilibrium position of the screen body, in the centre of mass S_o, there is a right-handed system of *x, y, and z* coordinate axes. The angles of rotation of the solid around individual axes are marked by φ_x, φ_y, φ_z, respectively. The sieve frame suspended in this way had 6 degrees of freedom in space. The simulation has been realized using the stiff element method, when each part was been treated as a rigid finite element. The individual parts have been linked with bond contact element (sieve with vibrator bases), rotational joints (vibrator bases with vibrator inertials) or elastic joints (sieve with ground) with constant values of stiffness and damping (very small values to provide numerical stability of solving process). Simulation model of movable sieve (Figure 6) comprised the upper solid plate 1 being grounded. The movable plate 2 modeling sieve frame was hanged on the four spring 3 linked to the plate 1. The bases B1, B2, and B3 of vibrators were bonded to the movable plate 2. The axes A1, A2, A3 were linked virtually to the base of vibrators, respectively. Inertials I1, I2, and I3 were joined rotationally with axes A1, A2, A3 with the same eccentricity relative to these corresponding axes and cannot move along the axes. Rotational speed of inertials relative to the corresponding axes have values according to the case of compared experimental cases. The spring 3 were characterized by stiffness and damping coefficient with directional component values according to the axes X, Y and Z.

2.3.2. The mathematical model of the staggering and circulating screen

The simulation model comprised also the mathematical model of movable sieve comprising the system of equations describing the free vibrations of the modelled system was determined. The vector of displacements of the sieve frame was determined from equation (4):

$$\underline{\boldsymbol{s}} = \left\{x, \varphi_x, y, \varphi_y, z, \varphi_z\right\}^T, \qquad (4)$$

where the symbol *T* denoted vector transposition operator.

The inertia matrix $\underline{\underline{\boldsymbol{B}}}$ of the considered system was in the form (5):

$$\underline{\underline{\boldsymbol{B}}} = \begin{bmatrix} M & & & & & 0 \\ & I_x & & & & \\ & & M & & & \\ & & & I_y & & \\ & & & & M & \\ 0 & & & & & I_z \end{bmatrix}, \qquad (5)$$

The elasticity matrix $\underline{\underline{\boldsymbol{K}}}$of the system had coefficients determined, for example, experimentally or using the finite element method for the modelled system.

The system of six equations of free motion of the sieve frame based on Newton's second law of dynamics in the matrix notation had the form (6):

$$\underline{\underline{\boldsymbol{B}}} \cdot \underline{\ddot{\boldsymbol{s}}} + \underline{\underline{\boldsymbol{K}}} \cdot \underline{\boldsymbol{s}} = \underline{\boldsymbol{0}}, \qquad (6)$$

Equation (6) was a homogeneous equation that was part of the full equation of motion of the system under consideration. To determine the elasticity matrix $\underline{\underline{\boldsymbol{K}}}$coefficients in equation (6), the sieve frame was deflected from the equilibrium position, giving it successively displacements following the positive returns of the individual six degrees of freedom. The positions of the body after a deflection from the equilibrium position are marked in Figure 6 with a dotted line.

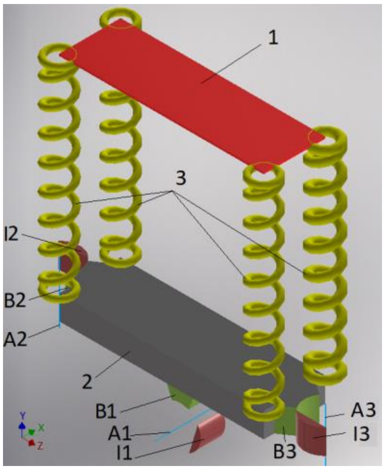

Fig. 6. The positions of the sieve frame at and after a deflection from the equilibrium position

Each deflection of the solid from the equilibrium position was accompanied by the appearance of reactive forces in the elastic elements of the system. These forces and their moments, through the elements of the system's elasticity matrix $\underline{\underline{\boldsymbol{K}}}$in equation (6), were dependent on the respective deflections. The elasticity coefficients can be estimated by knowing the elasticity constants of the elastic elements supporting the screen body. By modelling the sieve frame as a set of finite elements of the SOLID type with very high stiffness, suspended on bars treated as flexible elements of the LINK type connected to this cuboid and the ground through nodes / spherical joints with six degrees of freedom, it was possible to determine the eigenfrequencies α_i of the system in the directions consistent with the modal analysis using the finite element method. The stiffness coefficients are determined from the relationship (7):

$$K_i = \begin{cases} m_i \alpha_i^2 & for\ i = x, y, z \\ I_i \alpha_i^2 & for\ i = \varphi_x, \varphi_y, \varphi_z \end{cases}, \qquad (7)$$

The movement of the screen was forced due to the operation of inertial vibrators driven by electric motors, generating centrifugal forces forcing component oscillatory movements. The vector$\underline{\boldsymbol{P}}$ of forces and moments of exciting forces acting on the considered dynamic system had the form (8).

$$\underline{\boldsymbol{P}} = \left\{P_x, M_x, P_y, M_y, P_z, M_z\right\}^T, \qquad (8)$$

The system of complete equations of the forced motion of the sieve frame had the form (9):

$$\underline{\underline{\boldsymbol{B}}} \cdot \underline{\ddot{\boldsymbol{s}}} + \underline{\underline{\boldsymbol{K}}} \cdot \underline{\boldsymbol{s}} = \underline{\boldsymbol{P}}, \qquad (9)$$

The expanded version of the system of complete equations of motion had the form (10):

$$M\ddot{x} + K_x x - K_x a_x \varphi_z = F_{x2} + F_{x3},$$
$$J_x \ddot{\varphi}_x + K_y b_1^2 \varphi_x + K_z a_0^2 \varphi_x + K_z a_0 z = -F_{z1} \cdot h_1 + F_{z2} \cdot \upsilon_2 + F_{z3} \cdot \upsilon_3$$
$$M\ddot{y} + K_y y = F_{y1} + F_{y2} + F_{y3}, J_y \ddot{\varphi}_y + K_x (b_0^2 + b_1^2) \varphi_y = -F_{x2} \cdot w_2 + F_{x3} \cdot w_3$$
$$M\ddot{z} + K_z z + K_z a_0 \varphi_x = F_{z1} + F_{z2} + F_{z3},$$

$$J_z\ddot{\varphi}_z + K_y b_0^2\varphi_z + K_x a_0^2\varphi_z + K_x a_0 x = -F_{x2}\cdot\upsilon_2 - F_{x3}\cdot\upsilon_{3,}\ (10)$$

The dimensions a_0, b_0, b_1, υ_2, υ_3, h_1, h_2, w_2 and w_3 were shown in Figure 7. The system of equations of motion was described by the relationship (11):

$$M\ddot{x} + K_x x - K_x a_0\varphi_z = m_2\rho_2\omega_2^2\cdot\cos\omega_2 t + m_3\rho_3\omega_3^2\cdot\cos\omega_3 t$$

$$I_x\ddot{\varphi}_x + K_y b_1^2\varphi_x + K_z a_0^2\varphi_x + K_z a_0 z = h_1 m_1\rho_1\omega_1^2\cos\omega_1 t + \upsilon_2 m_2\rho_2\omega_2^2\sin\omega_2 t - \upsilon_3 m_3\rho_3\omega_3^2\sin\omega_3 t$$

$$M\ddot{y} + K_y y = m_1\rho_1\omega_1^2\sin\omega_1 t + m_2\rho_2\omega_2^2\sin\omega_2 t + m_3\rho_3\omega_3^2\sin\omega_3 t$$

$$J_y\varphi_y + K_x(b_0^2 + b_1^2)\varphi_y = -w_2 m_2\rho_2\omega_2^2\cos\omega_2 t + w_3 m_3\rho_3^2\cos\omega_3 t$$

$$M\ddot{z} + K_z z + K_z a_0\varphi_x = m_1\rho_1\omega_1^2\cos\omega_1 t,$$

$$J_z\ddot{\varphi}_z + K_y b_0^2\varphi_z + K_x a_0^2\varphi_z - K_x a_0 x = h_2 m_2\rho_2\omega_2^2\cos\omega_2 t + \upsilon_3 m_3\rho_3\omega_3^2\cos\omega_3 t$$

(11)

Equation (11) presented a system of six ordinary differential equations with constant non-homogeneous coefficients. The solution allowed for the determination of the kinematic parameters of the screen movement. The solution of such a system of differential equations was obtained numerically.

2.2.3 The grain's throwing coefficient

The solution of the screen motion equations allowed for the analytical determination of the grain's throwing coefficient. That coefficient was used to determine the ratio of the maximum inertia force acting in a given direction on a mass element to the component of the gravity force of this element in the same direction for various directions of displacement. After considering the inclination angle of the screen (angle αn in Fig. 5), the grain's throwing coefficient calculated during simulation generally marked as W accepted the specific marks:

- W_n (12) for direction "n" normal to the sieve surface (Figure 8):

$$W_n = \frac{(P_{bn})_{max}}{G_n} = \frac{(a_n)_{max}}{g_n} = \frac{\left(\frac{d^2y}{dt^2}\right)_{max} cos\alpha + \left(\frac{d^2z}{dt^2}\right)_{max} sin\alpha}{g cos\alpha},\ (12)$$

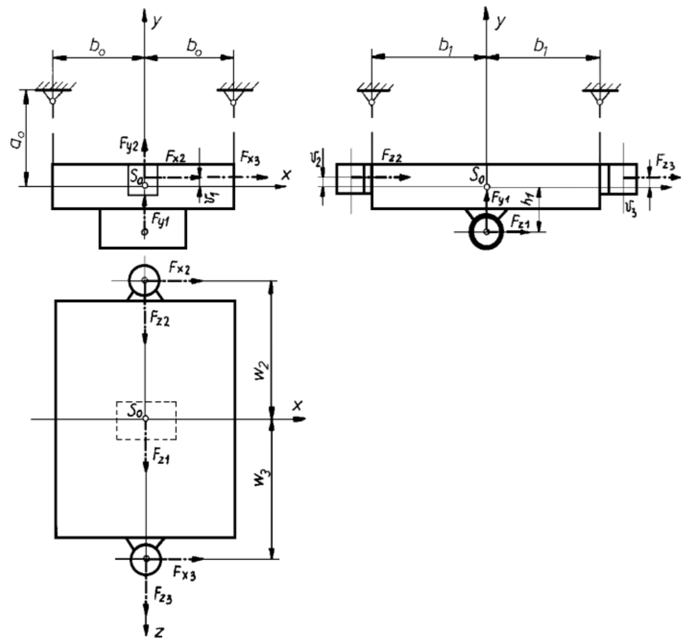

Fig. 7. The characteristic dimensions for the mathematical model of the oscillating sieve frame.

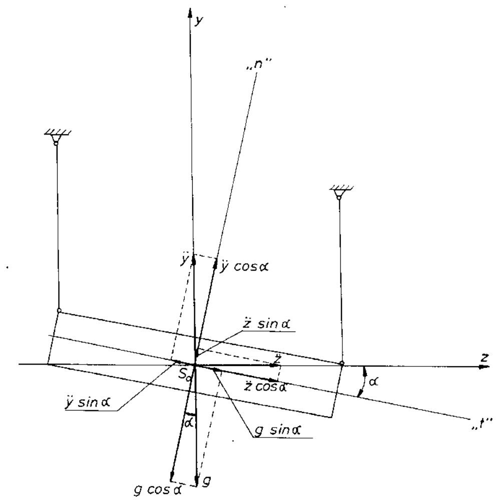

Fig. 8. The grain's throwing directions considered during the simulation.

- W_t (13) for the tangential direction "t" to the sieve surface (Figure 8):

$$W_t = \frac{(P_{bt})_{max}}{G_t} = \frac{(a_t)_{max}}{g_t} = \frac{\left(\frac{d^2y}{dt^2}\right)_{max} sin\alpha + \left(\frac{d^2z}{dt^2}\right)_{max} cos\alpha}{gsin\alpha}, (13)$$

3. Results and Discussion

3.1. Trajectories

The exemplary trajectories of the sieve frame centre of the gravity in individual planes of the reference system for the tested cases of excitation force generated by vibrators with the parameters including masses of the vibrator inertials m_1=m_2=m_3=0.2 kg, and distances of the vibrator inertials from vibrator rotor axes ρ_1=ρ_2=ρ_3=0.07 m, and with the configuration of the rotational speed, where their modules were equal to $|w_1| = |w_2| = |w_3|$=146 rad/s were shown in Figures:

9a – obtained from the experiment, 9b – obtained from simulation, for Configuration 1 of vibrator rotational speeds: $w_2 = w_3, w_1 = 0$,

10a - obtained from the experiment, 10b – obtained from simulation, for Configuration 2 of vibrator rotational speeds: $w_2 = -w_3, w_1 = 0$,

11a - obtained from the experiment, 11b – obtained from simulation, for Configuration 3 of vibrator rotational speeds: $w_2 = w_3 = w_1$,

12a - obtained from the experiment, 12b – obtained from simulation, for Configuration 4 of vibrator rotational speeds: $w_2 = -w_3 = w_1$,

13a - obtained from the experiment, 13b – obtained from simulation, for Configuration 5 of vibrator rotational speeds: $w_2 = w_3 = 0, w_1 \neq 0$.

For each Configuration, Figures contained trajectories obtained in XZ plane, YZ plane and XY plane, placed from top to the bottom.

The obtained from experiment amplitudes A_X, A_Y, and A_Z of oscillations of the sieve frame centre of the gravity in directions of axes x, y, z, respectively, were shown in Table 1.

Tab. 1. Amplitudes of oscillations obtained from measurements.

Configuration number	A_X [mm]	A_Y [mm]	A_Z [mm]
1	0.868±0.046	0.452±0.046	0.750±0.346
2	0.930±0.005	0.930±0.001	0.187±0.059
3	0.853±0.051	0.225±0.085	0.443±0.196
4	0.850±0.075	0.512±0.008	0.382±0.267
5	0.243±0.055	0.492±0.019	0.687±0.092

For all configurations of vibrator rotational speeds, all oscillation amplitudes were below 1. The highest values of the A_X and A_Y amplitudes occurred for Configuration 2, and of the A_Z amplitude for Configuration 1. The lowest value of the A_X amplitude was obtained for Configuration 5, the A_Y amplitude for Configuration 3 and the A_Z amplitude for Configuration 2. For the configurations from 1 to 4 the A_X amplitudes were greater than the other ones. For Configuration 1 of vibrator rotational speed the amplitude of oscillating motion in the Y direction obtained from the experiment was 5-10% higher compared to that from the simulation. The amplitude of oscillations in the X direction obtained from the experiment was up to 10 % higher than that from the simulation. The greatest differences between amplitudes of oscillation obtained from measurement and simulation were observed for the Z direction. It could be caused by the non-symmetric distribution of mass and elasticity parameters relative to the XY symmetry plane of the real riddle. The inclination of the nearly elliptical shape of the trajectory measured for the centre of gravity of the real riddle could point to the occurrence of damping in the XZ plane. The irregular shapes of trajectories obtained from the simulation pointed out the important role of initial conditions. The shapes of movements in the XY and YZ planes, and to a lesser extent in the

XZ plane, obtained from the measurement, are close to an ellipse and contribute to good segregation of the granular layer on the screen.

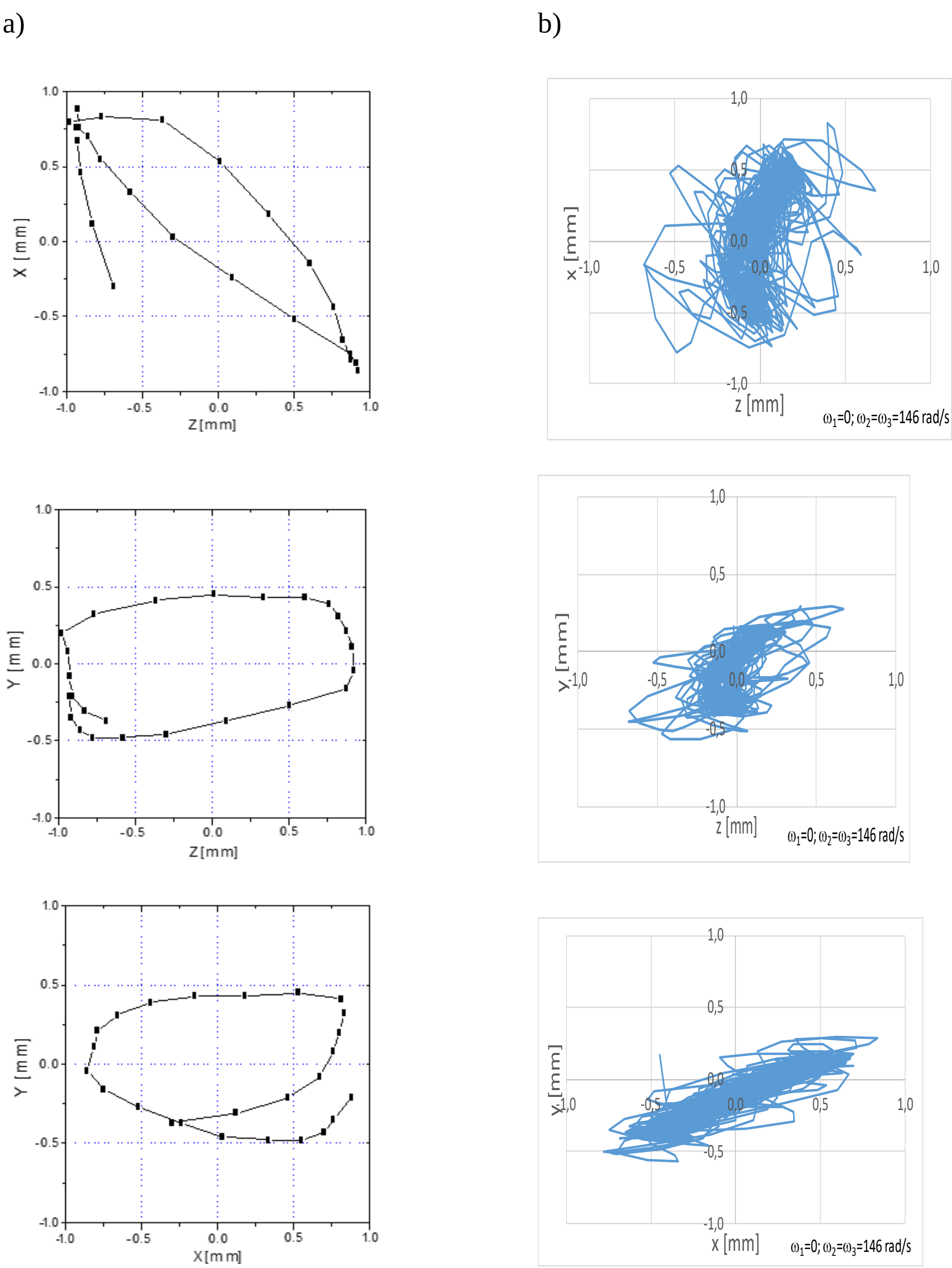

Fig. 9. Trajectories of the sieve frame center of the gravity for Configuration 1 of vibrator rotational speed; a) obtained from experiment; b) obtained from simulation.

However, the simulation results only indicate the possibility of intensive mixing of grains in the XZ plane.

a) b)

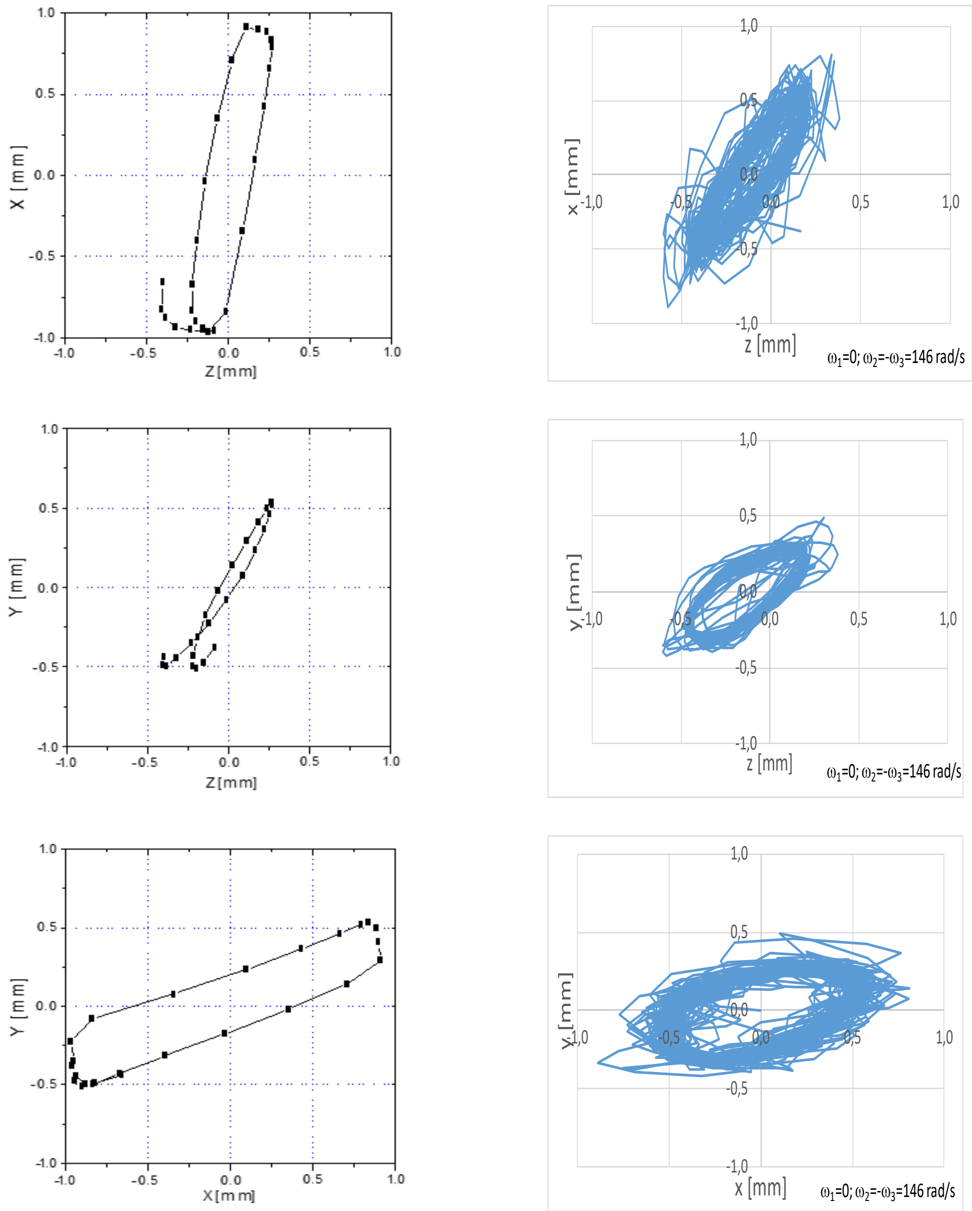

Fig. 10. Trajectories of the sieve frame center of the gravity for Configuration 2 of vibrator rotational speed; a) obtained from experiment; b) obtained from simulation.

For Configuration 2 of vibrator rotational speeds, the amplitude of oscillations in the X direction obtained from the experiment was about 10 % higher than that from the simulation. The differences between amplitudes of oscillation obtained from measurement and simulation observed both for the Y and Z directions were even lower. For the Z direction, such differences were greater. It also could be caused by the non-symmetric distribution of mass and elasticity parameters relative to the XY symmetry plane of the real riddle and relative to the ZX one, however to a smaller extent. The irregular shapes of trajectories obtained from the simulation pointed out the important role of initial conditions. Ellipse-like shapes of movements in the XY and XZ planes obtained from the experiment are narrower than in the previous case, which is why there may be a much lower intensity of granular layer segregation on the sieve. The results of the simulation indicate also a possibility of such segregation.

a) b)

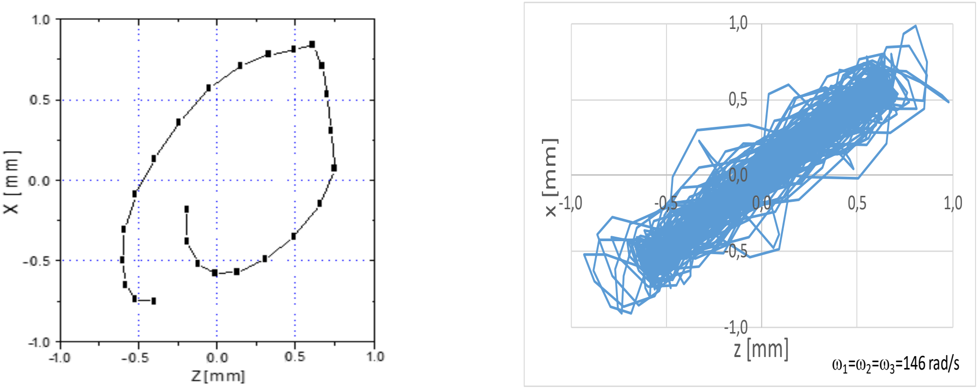

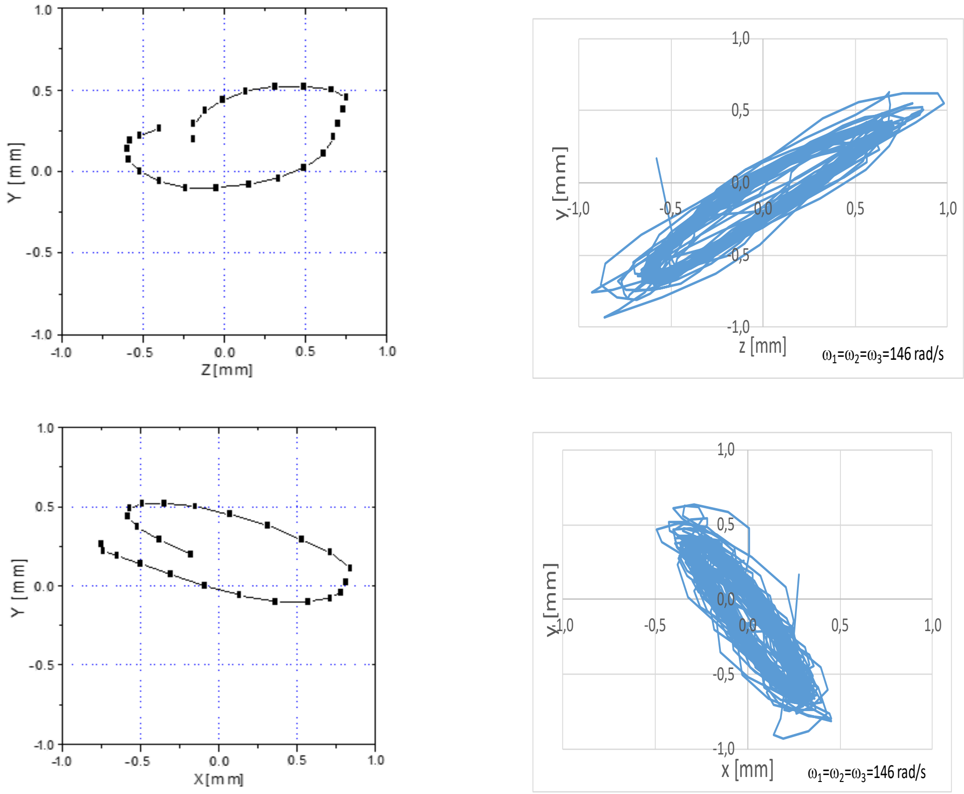

Fig. 11. Trajectories of the sieve frame center of the gravity for Configuration 3 of vibrator rotational speed; a) obtained from experiment; b) obtained from simulation

For Configuration 3 of vibrator rotational speeds, the amplitudes of oscillations in the X direction obtained from the experiment were about 20 % lower than that from the simulation. In the Y direction, the amplitudes of oscillations obtained from the experiment were lower by 10-30 % compared to that from the simulation. In the Z direction, the amplitudes of oscillations were 10-20% lower than those from the simulation. It also could result from the non-symmetric distribution of mass and elasticity parameters relative to the XY symmetry plane of the real riddle and relative to the ZX one. The inclination of the nearly elliptical shape of the trajectory measured for the centre of gravity of the real riddle could point to the occurrence of damping in the XZ plane. Also here, the irregular shapes of trajectories obtained from the simulation pointed out the important role of initial conditions.

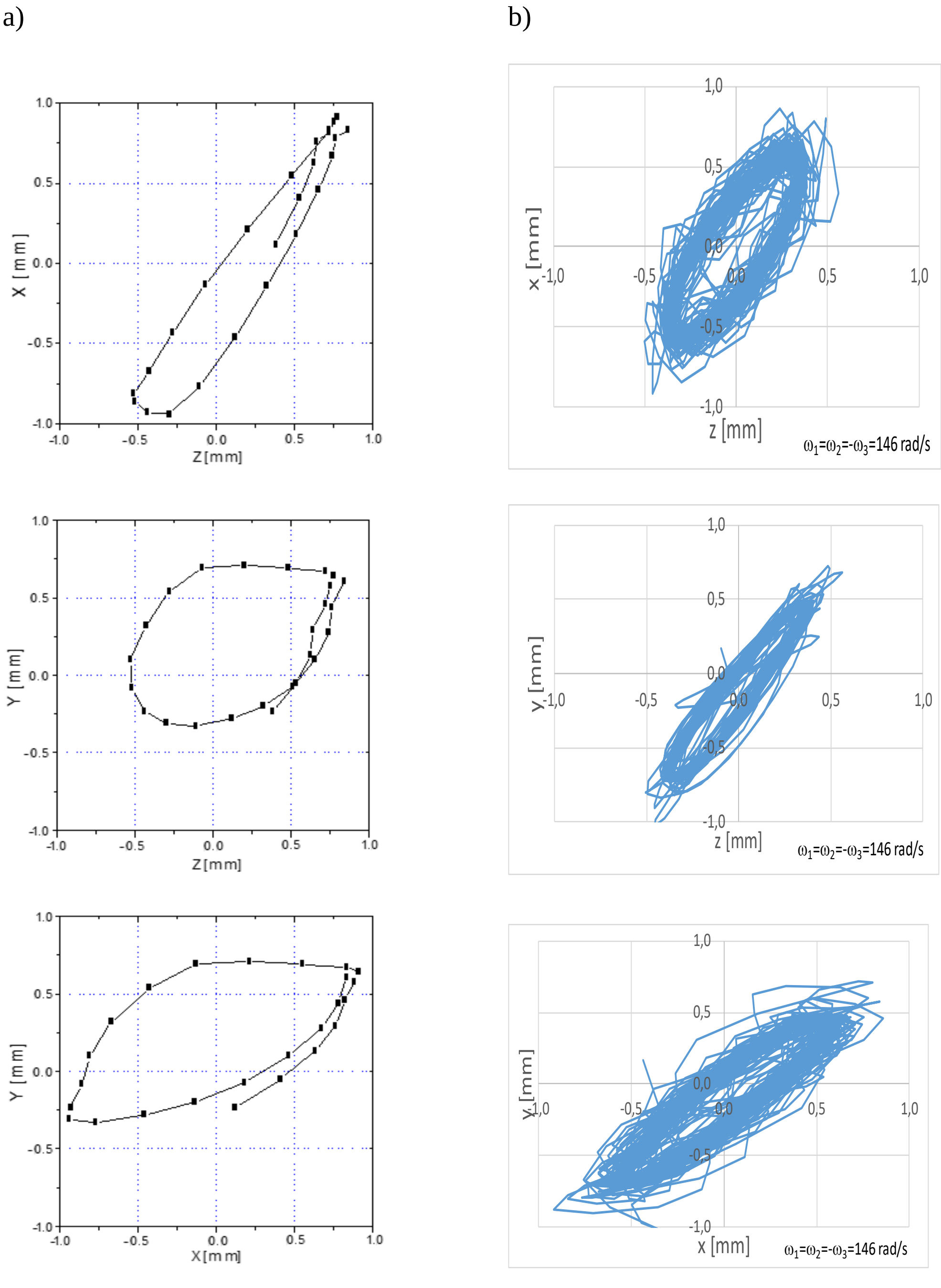

Fig. 12. Trajectories of the sieve frame center of the gravity for Configuration 4 of vibrator rotational speed; a) obtained from experiment; b) obtained from simulation.

Similarly, to the case of Configuration 1 of vibrator rotational speeds, the shapes of movements in the XY and YZ planes, and the XZ plane, obtained from the measurement, are close to an ellipse and contribute to good segregation of the granular layer on the screen. However, the obtained ellipses in XY and YZ planes were narrower. The resulting trajectories obtained from simulation also indicate the possibility of good segregation of the granular layer on the screen, however to less extent than those from an experiment. For Configuration 4 of vibrator rotational speeds, the amplitudes of oscillations in the X direction obtained from the experiment were 5-10 % higher than those from the simulation. In the Y direction, the amplitudes of oscillations obtained from the experiment were 5-30% lower compared to those from the simulation. Interestingly, the bias of the measured oscillations of the real riddle existed in the Y direction. In the Z direction, the amplitudes of oscillations were up to 20% higher than those from the simulation. It also could result from the non-symmetric distribution of mass and elasticity parameters relative to the XY symmetry plane of the real riddle and relative to the ZX one. The inclination of the nearly elliptical shape of the trajectory measured for the center of gravity of the real riddle could point to the occurrence of damping in the XZ plane, and a much smaller extent in two other planes. Once again, the irregular shapes of trajectories obtained from the simulation pointed out the important role of initial conditions. Similarly, to the case of Configuration 1 of vibrator rotational speeds, the shapes of movements in the XY and YZ planes, and to a less extent in the XZ plane, obtained from the measurement, are close to an ellipse and contribute to good segregation of the granular layer on the screen. However, the obtained ellipses in XY and YZ planes were narrower. The resulting trajectories obtained from simulation also indicate the possibility of good segregation of the granular layer on the screen, however to less extent than those from an experiment. For Configuration 5 of vibrator rotational speeds, the amplitude of oscillating motion in the Y direction obtained from the experiment was up to 10% higher compared to that from the simulation. The amplitude of oscillations in the X direction obtained from the experiment was about 30 % higher than that from the simulation. The differences between amplitudes of oscillations obtained from measurement and simulation were observed for the Z direction were up to 20%. It could be caused by the non-symmetric distribution of mass and elasticity parameters relative to the XY symmetry plane of the real riddle. Interestingly, the bias of the measured oscillations of the real sieve existed in all axes directions. Also here, the irregular shapes of trajectories obtained from the simulation emphasized the important role of initial conditions. Ellipse-like shapes of movements in the XY and YZ planes obtained from the experiment are narrower than in the case of Configuration 1 of vibrator rotational speeds, which is why there may be a much lower intensity of granular layer segregation on the sieve. The results of the simulation indicated the possibility of an intensive mixing of mixing the granular layer on the sieve only in the YZ plane.

a)

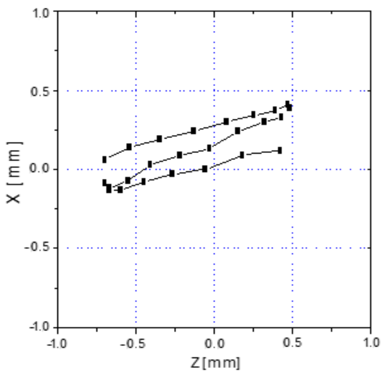

b)

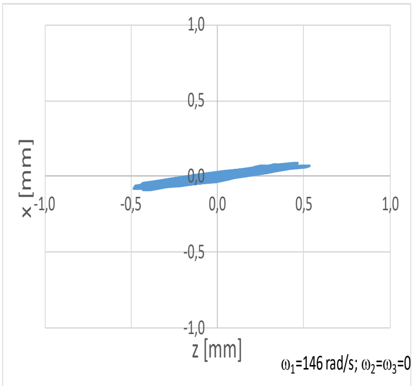

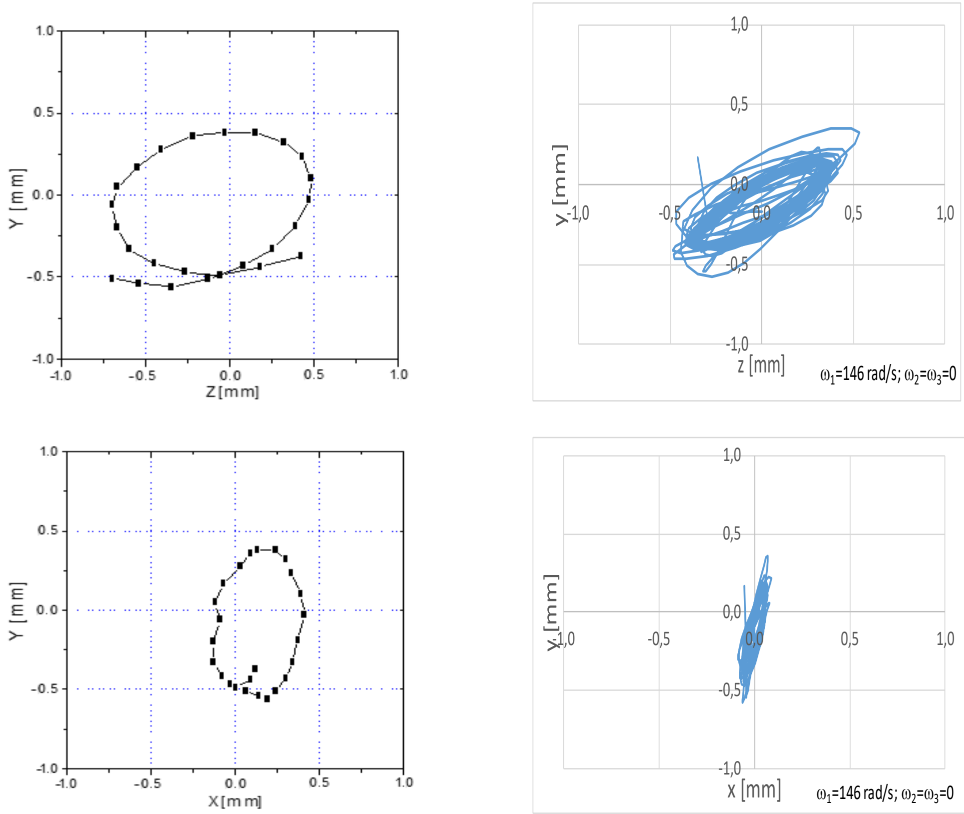

Fig. 13. Trajectories of the sieve frame center of the gravity for Configuration 5 of vibrator rotational speed; a) obtained from experiment; b) obtained from simulation

3.2 The grain's throwing coefficient

The values obtained from the experiment for the grain's throwing coefficients K_Y and K_Z for the consecutive configurations of vibrator rotational speeds were shown in Table 2. The values obtained from the simulation for the grain's throwing coefficients W_t and W_n for the mentioned configurations of rotational speeds were presented in Table 3. All values of such coefficients were obtained for the angle α of the sieve inclination equal to 15°.

Tab. 2. The values obtained from the experiment for grain's throwing coefficients K_Y and K_Z

Configuration number	K_Y [-]	K_Z [-]
1	1.023 ± 0.103	6.346 ± 2.933
2	2.110 ± 0.001	1.580 ± 0.501
3	0.510 ± 0.190	3.763 ± 1.651
4	1.163 ± 0.015	3.233 ± 2.255
5	1.117 ± 0.042	5.810 ± 0.787

The resulting values of the grain's throwing coefficient K_Y obtained from the experiment were below 1 for Configuration 3 of vibrator rotational speed, which practically meant no detachment of the granular product from the sieve. That could sometimes also occur for Configuration 1. The maximal values of such a coefficient occurred for Configuration 2. The resulting values of the grain's throwing coefficient K_Z were above 1 for all configurations of vibrator rotational speeds considered during experiments. The highest values occurred for Configuration 1, and the lowest ones for Configuration 2. The values of the resultant grain's throwing coefficient K_R were above 3 in all experimental cases, which indicated a high possibility of ensuring the toss of the granular mass on the sieve, which is favourable from the point of view of mixing the sieved mass [20, 26].

Table 3. *The values obtained from simulation for grain's throwing coefficients W_n and W_t*

Configuration number	W_n [-]	W_t [-]
1	1.04	6.21
2	1.14	4.83
3	2.06	9.45
4	1.78	5.47
5	1.35	5.04

The resulting values of the grain's throwing coefficient W_n obtained from the simulation were above 1 for all configurations of vibrator rotational speeds, which practically provided a detachment of the granular mass from the sieve. The maximal values of such a coefficient occurred for Configuration 3. Also for Configuration 1, it was obtained high values of the coefficient W_n, were greater by up to 80% compared to the other configurations. The resulting values of the grain's throwing coefficient W_t were above 1 for all configurations analyzed during simulations. The highest values occurred for Configuration 3, and the lowest ones for Configuration 2. The values of the resultant grain's throwing coefficient W_R calculated from simulation were above 3 for all analyzed configurations, which also indicated good possibilities of ensuring the toss of the granular product on the sieve, which is favourable from the point of view of mixing the sieved mass [20, 26].

There has been a considerable amount of research into improving the efficiency and capacity of vibrating screens. In one study [27], a 3D model of a vibratory screen was created and a multi-body dynamic simulation was used to determine the basic operating parameters of the screen. The results of the simulation were the subject of verification by experiment. According to the literature, it is a common practice to optimize the vibration parameters of a vibratory screen by means of simulation. The results of simulation can provide a theoretical basis for the optimization of the parameters of the working conditions of vibrating screens, such as those with variable rectangular hole screens [28] or those with kneading devices [29].

4. Conclusions

Based on the results obtained from experiments and simulations some conclusions can be formulated.

1. The reeling and circulating sifter provided an interesting device to ensure intensive on-sieve mixing of the screened granular mass.

2. For a fixed value of the sieve inclination angle close to 15° the obtained values of the resultant grain’s throwing coefficient, obtained both from the experiment and the simulation, indicate the detachment of the granular mass from the sieve, which is favourable from the point of view of the sieving process.

3. For the configuration of vibrator rotational speeds of $w_2 = w_3$ and $w_1 \neq 0$, and more seldom for that of $w_2 = w_3$ and $w_1 = 0$ no detachment of the granular mass from the sieve can occur.

4. The elliptical or close to elliptical shapes of movements in the XY and YZ planes, and in the XZ plane, obtained from the measurement, contribute to good segregation of the granular layer on the screen, especially for the configurations of the vibrator rotational speeds including that of $w_2 = w_3$ and $w_1 = 0$, that of $w_2 = -w_3$ and $w_1 = 0$, and that of $w_2 = w_3$ and $w_1 \neq 0$.

5. The visible differences between trajectories of the centre of gravity of the vibrating sieve obtained from the experiment and simulation could result from the non-symmetric distribution of mass and elasticity parameters relative to the XY symmetry plane of the real vibrating sieve. Also, vibrators could be mounted non exactly symmetrically against such a plane. Their weights could also be not precisely symmetrically distributed causing temporary nonsymmetrical or non-antisymmetric character of excitations relative to the XY symmetry plane. 6.For rotational speed configurations with $w_2 = -w_3$ enabling reverse synchronization of external vibrators and for a fixed sieve inclination angle, by controlling the rotational speed w_1 of the central vibrator, distances of its inertials from vibrator rotor axis ρ_1, and their mass m_1, it is possible to obtain the desired trajectories of screened product grains recommended for processes carried out with the use of specialized machines, for example, gutter pelletizers.

Part of this research was funded by the state budget under the subsidy of the Ministry of Science and Higher Education Republic of Poland (No. 00/BCS/08/00/1/3/0284). The study presented in this paper was carried out as part of research 501/9-9-1-933.

References

[1] Gursky V.R., Kuzio I., Krot P., Zimroz R.: *Energy-Saving Inertial Drive for Dual-Frequency Excitation of Vibrating Machines*, Energies, 14, 1, 71, 2021. https://doi.org/10.3390/en14010071.

[2] Kumar D., Kumar D.: Chapter 4 - Coal Sizing. Kumar, D., Kumar, D. (eds.), *Sustainable Management of Coal Preparation*. Woodhead Publishing, Walnut, St Philadelphia, PA, USA, 2018, pp. 49–68.

[3] Wills B.A., Finch J.A.: Chapter 8 -Industrial Screening. Wills, B.A., Finch, J.A., (eds.), *Wills' Mineral Processing Technology*, 8th ed. Butterworth-Heinemann, Oxford, UK, 2016, pp.181–197.

[4] Simonyan K.J., Yiljep Y.: *Investigating grain separation and cleaning efficiency distribution of a conventional stationary rasp-bar sorghum thresher*. Agric. Eng. Int. CIGR Ej. 10, 2008, pp. 1–10.

[5] Aipov R., Linenko A., Badretdinov I., Tuktarov M., Akchurin S.: *Research of the work of the sieve mill of a grain-cleaning machine with a linear asynchronous drive*. Math. Biosci. Eng. 17, 4, 2020, pp. 4348–4363, DOI:10.3934/mbe.2020240.

[6] Giyevskiy A.M., Orobinsky V.I, Tarasenko A.P., Chernyshov A.V., Kurilov D.O., *Substantiation of basic scheme of grain cleaning machine for preparation of agricultural crops seeds*. IOP Conf. Ser. Mater. Sci. Eng. 327, 4, 2018. DOI:10.1088/1757-899X/327/4/042035.

[7] Vasylkovskyi O., Vasylkovska K., Moroz S., Sviren M., Storozhyk L.: *The influence of basic parameters of separating conveyor operation on grain cleaning quality*. INMATEH, 57, 1, 2019, 63–70, https://doi.org/10.35633/INMATEH_57.

[8] Ma L., Song X., Wang H., Xu X., Han T., Guo H.: *Screening Kinematics Analysis of Cleaning Organs, and Extractives*. IOP Conf. Ser. Mater. Sci. Eng. 452, 4, 04212, 2018. DOI:10.1088/1757-899X/452/4/042123.

[9] Shevtsov I.V., Beznosov V.A.: Drive unit for sieve mills of grain cleaning machines. *Agrar. Vestn. Ural.* 2, 2014, pp. 43–45.

[10] Aradwad P.P., Sinha J.P., Kumar T.V.A., Yadav R.S., Samuel D.V.K,: *Development of solar powered screen cleaner*. Indian J. Agric. Sci. 88, 12, 2018, pp. 1914–1919.

[11] Yarullin R., Aipov R., Gabitov I., Linenko A., Akchurin S., Mudarisov S., Khasanov E., Rakhimov Z., Masalimov I.: *Adjustable driver of grain cleaning vibro-machine with vertical axis of eccentric masses rotation*. J. Eng. Appl. Sci., 13, 8SI, 2018, pp. 6398–6406, DOI:10.36478/jeasci.2018.6398.6406.

[12] Linenko A.V., Gabitov I.I., Baynazarov V.G., Tuktarov M.F., Aipov R.S,, Akchurin S.V, Kamalov T.I., Badretdinov I.D., Leontiev D.S., Vokhmin V.S.: *The mechatronic module "linear electric drive—sieve boot" intelligent control system of grain cleaner*. J. Balk. Tribol. Assoc., 25, 3, 2019, pp. 708–717.

[13] Neyman L.A., Neyman V.Y.: *Dynamic model of a vibratory electromechanical system with spring linkage.* In Proceedings of the 2016 11th International Forum on Strategic Technology, IFOST, Novosibirsk, Russia, 1–3 June 2016, pp. 23–27.

[14] Lawinska K., Modrzewski R.: *Analysis of sieve holes blocking in a vibrating screen and a rotary and drum screen.* Physicochem. Probl. Miner. Process. 53, 2017, pp.812–828.

[15] Li H., Li Y., Guo F., Zhao Z., Xu L.: *CFD–DEM simulation of material motion in air-and-screen cleaning device.* Comput. Electron. Agric., 88, 2012, pp. 111–119, DOI:10.1016/j.compag.2012.07.006.

[16] Li H., Li Y., Tang Z., Xu L., Zhao Z.: *Numerical simulation and analysis of vibration screening based on EDEM.* Trans. *CSAE*, 27, 5, 2011, pp. 117–121, DOI:10.3969/j.issn.1002-6819.2011.05.019.

[17] Elskamp F., Kruggel-Emden H., *DEM simulations of screening processes under the influence of moisture.* Chem. Eng. Res. Des., 136, 2018, pp. 593–609, DOI:10.1016/j.cherd.2018.06.022.

[18] Elskamp F., Kruggel-Emden H.: *Extension of process models to predict batch screening results under the influence of moisture based on DEM simulations*. Powder Technol., 342, 2019, pp. 698–713, DOI:10.1016/j.powtec.2018.10.039.

[19] Yan H., Li Y., Fuan F., Peng F., Yang X., Hou X.: *Analysis of the Screening Accuracy of a Linear Vibrating Screen with a Multi-layer Screen Mesh.* Stroj. Vestn. J. Mech. Eng., 66, 5, 2020, pp. 289–299, DOI:10.5545/sv-jme.2019.6523.

[20] Peng L., Feng H., Wang Z., Wang H., Yang H., Huang H.: *Screening Mechanism and Properties of a Cantilevered Vibrating Sieve for Particles Processing.* Appl. Sci., 9, 22, 4911, 2019, DOI: 10.3390/app9224911.

[21] Szufa S., Piersa P., Junga R., Blaszczuk A., Modlinski N., Marczak-Grzesik M., Sobek S., Adrian L., Dzikuc M.: *Numerical modeling of the co-firing process of an in-situ steam-torrefied biomass with coal in a 230 MW industrial-scale boiler.* Energy, vol. 263E, 2023, 125918, DOI: 10.1016/j.energy.2022.125918

[22] Rostocki A., Ławińska K., Modrzewski R., Siegień G., Hejft R., Obraniak A., *Methods for Treatment of Animal and Plant-Based Biomass Waste,* Fibers Text. East. Eur. 30, 4, 2022, pp. 32-42. DOI: 10.2478/ftee-2022-0031

[23] Piersa P., Szufa S., Czerwińska J., Ünyay H., Adrian Ł., Wielgosinski G., Obraniak A., Lewandowska W., Marczak-Grzesik M., Dzikuć M., Romanowska-Duda Z., Olejnik T.P.: *Pine Wood and Sewage Sludge Torrefaction Process for Production Renewable Solid Biofuels and Biochar as Carbon Carrier for Fertilizers*. Energies, 14, 23, 8176, 2021, DOI: 10.3390/en14238176.

[24] Li L., Chen X.: *Multi-frequency Vibration Synchronization and Stability of the Nonlinear Screening System.* IEEE Access, 7, 2019, pp. 171032-171045, DOI:10.1109/ACCESS.2019.2955980.

[25] Liu Y., Meng G., Suo S., Li D., Wang A., Cheng X., Yang J.: *Spring Failure Analysis of Mining Vibrating Screens: Numerical and Experimental Studies.* Appl. Sci., 9, 16, 3224, 2019, DOI: 10.3390/app9163224.

[26] Lawinska K., Wodzinski P., Modrzewski R.: *Verification of the mathematical model of the screen blocking process*, Powder Technol. 256, 2014, pp. 506-511.
[27] Dang T.N.: *Modeling and Dynamic Simulation of a Multi-slope Vibrating Screen to Determine the Basic Working Parameters.* In: Nguyen, D.C., Vu, N.P., Long, B.T., Puta, H., Sattler, KU. (eds) Advances in Engineering Research and Application. ICERA 2022. Lecture Notes in Networks and Systems, 602. Springer, Cham. 2023 DOI:10.1007/978-3-031-22200-9_72
[28] Sun T., Wu B., Zhang H., Han Y., Liu H., Zhang Y.: *Discrete element simulation of particle flow and separation in a vibrating screen with variable rectangular hole screen*, Powder Technol. 434, 119305, 2024, DOI: 10.1016/j.powtec.2023.119305
[29] Tian S., Wang Y., Zhao W., Zhang Q., Wang S., Lang J., Xia R., Song J., Song W., *Comparative study on the screening performance of a vibrating screen with and without a kneading device, based on the discrete element method*, Powder Technol. 434, 119301, 2023, DOI: 10.1016/j.powtec.2023.119301.

dr inż. Dorota Gendaszewska – jest absolwentką Wydziału Biotechnologii i Nauk o Żywności Politechniki Łódzkiej. W 2015 roku obroniła pracę doktorską pt.: „Biodegradowalność i usuwanie imidazoliowych cieczy jonowych ze ścieków". Obecnie pracuje na stanowisku Lidera Obszaru w Łukasiewicz – Łódzkim Instytucie Technologicznym.

ORCID 0000-0002-9909-0880

dr inż. Magdalena Kłonowska – doktor nauk technicznych w dyscyplinie włókiennictwo, adiunkt w Instytucie Włókiennictwa, Wydział Technologii Materiałowych i Wzornictwa Tekstyliów Politechniki Łódzkiej

dr inż. Gabriela Kosiuk - ukończyła studia doktoranckie na Wydziale Technologii Materiałowych i Wzornictwa Tekstyliów Politechniki Łódzkiej w dyscyplinie Inżyniera Materiałowa. Jest laureatką IV Edycji Konkursu im. Profesora Żurka na najlepszą pracę dyplomową o tematyce włókienniczej. Zajmuje się problematyką wiedzy w zakresie geometrycznej struktury powierzchni tkanin. Obecnie pracuje w Instytucie Technologii Bezpieczeństwa "MORATEX" w Laboratorium Badań Metrologicznych.

ORCID 0000-0003-3029-9982

dr inż. Maciej Kuchar ukończył studia w roku 1992 na Wydziale Mechanicznym Politechniki Łódzkiej. W 2003 r. uzyskał stopień doktora na Politechnice Łódzkiej. Jest zatrudniony na stanowisku starszego wykładowcy w Politechnice Łódzkiej w Katedrze Pojazdów i Podstaw Budowy Maszyn. Dziedzina naukowa: Inżynieria Mechaniczna. Zajmuje się zagadnieniami budowy i eksploatacji maszyn i urządzeń, w szczególności włókienniczych, oraz analizami naprężeń w materiałach.

dr hab. inż. Katarzyna Ławińska – Dyrektor Centrum B+R w Łukasiewicz - Łódzkim Instytucie Technologicznym. Kierownik projektów, w tym LIDER, Miniatura, Eureka, NdS oraz inwestycyjnych. Działalność: inżynieria chemiczna i materiałowa oraz inżynieria środowiska, górnictwo i energetyka. ORCID 0000-0002-0064-3159. Zainteresowania B+R: innowacyjne rozwiązania w sektorze TCLF, zagospodarowanie odpadów, bezpieczeństwo produktów, monitoring środowiska oraz technologie rolno-spożywczych.

prof. dr hab. inż. Małgorzata Matusiak - profesor w dziedzinie nauk inżynieryjno-technicznych w dyscyplinie inżynieria materiałowa. Pracownik badawczo-dydaktyczny Politechniki Łódzkiej, Wydział Technologii Materiałowych i Wzornictwa Tekstyliów, Instytut Architektury Tekstyliów.

mgr Katarzyna Miśkiewicz - jest absolwentką Wydziału Biologii i Ochrony Środowiska Uniwersytetu Łódzkiego. Obecnie pracuje na stanowisku Starszego Specjalisty w Łukasiewicz – Łódzkim Instytucie Technologicznym.

ORCID 0000-0002-5034-1829

dr hab. inż. Remigiusz Modrzewski w roku 1994 ukończył studia na Wydziale Inżynierii Procesowej i Ochrony Środowiska Politechnice Łódzkiej. W 2000 roku uzyskał stopień doktora, a w 2021 doktora habilitowanego. Jest zatrudniony na stanowisku adiunkta w Politechnice Łódzkiej w Katedrze Inżynierii Chemicznej. Jest współautorem ponad 80 publikacji naukowych. Jego zainteresowania badawcze obejmują modelowanie procesu przesiewania i granulacji materiałów ziarnistych oraz projektowanie i budowę przesiewaczy przemysłowych.

dr hab. inż. Andrzej Obraniak ukończył studia w roku 1989 na Wydziale Mechanicznym Politechniki Łódzkiej. W 2002 r. uzyskał stopień doktora zaś w 2020 roku stopień doktora habilitowanego na Wydziale Inżynierii Procesowej i Ochrony Środowiska Politechniki Łódzkiej. Jest profesorem uczelni w Katedrze Inżynierii Chemicznej na Wydziale Inżynierii Procesowej i Ochrony Środowiska Politechniki Łódzkiej. Dziedzina naukowa - inżynieria chemiczna. Prowadzi badania dotyczące procesu granulacji i otoczkowania.

prof. dr hab. inż. Tomasz P. Olejnik – jest pracownikiem naukowo-dydaktycznym na Wydziale Biotechnologii i Nauk o Żywności Politechniki Łódzkiej, zatrudnionym na stanowisku profesora w Katedrze Cukrownictwa i Zarządzania Bezpieczeństwem Żywności. Posiada tytuł profesora w naukach technicznych w dyscyplinie ochrona środowiska, górnictwo i energetyka. Aktualnie prowadzi badania naukowe obejmujące biotechnologię, technologię żywności oraz inżynierię procesową. Tematyka badawcza obejmuje między innymi: modelowanie procesów jednostkowych w przetwórstwie surowców mineralnych i spożywczych (rozdrabnianie, klasyfikację, granulowanie, mieszanie); transport masy i energii w tym modelowanie strumieni masy i energii (narzędzia CFD); optymalizację technologiczną przetwórstwa żywności wraz z optymalizacją konstrukcyjną maszyn i urządzeń. Jest autorem i współautorem blisko 200 publikacji w czasopismach zagranicznych i krajowych, w tym 87 publikacji z listy JCR. Lista publikacji obejmuje monografie oraz książki. Ponadto jest autorem licznych ekspertyz i rozwiązań technologicznych zamawianych przez zewnętrzne otoczenie uczelni. Autor 63 patentów oraz 10 zgłoszeń patentowych.

ORCID 0000-0001-6941-4111

dr hab. inż. Magdalena Orczykowska - ukończyła studia na Wydziale Inżynierii Procesowej i Ochrony Środowiska Politechniki Łódzkiej, na którym pracuje do chwili obecnej. Kierunek prowadzonych przez nią badań obejmuje zagadnienia związane z właściwościami reologicznymi, a zwłaszcza lepkosprężystymi biomateriałów stosowanych w przemyśle spożywczym, farmaceutycznym i kosmetycznym.

ORCID: 0000-0002-0109-2563

dr. inż. Adam Rylski ukończył studia i uzyskała stopień doktora na Wydziale Mechanicznym Politechnice Łódzkiej. Jest zatrudniony na stanowisku adiunkta w Instytucie Inżynierii Materiałowej na Wydziale Mechanicznym Politechniki Łódzkiej. Dziedzina naukowa: Inżynieria Materiałowa. Jest specjalistą od analiz materiałów, tribologii, cienkich warstw. Posiada szereg patentów i wyróżnień w swojej dziedzinie naukowej.

inż. Karolina Serafin – absolwentka kierunku studiów Włókiennictwo i Przemysł Mody na Wydziale Technologii Materiałowych i Wzornictwa Tekstyliów Politechniki Łódzkiej, studentka studiów II stopnia na kierunku Włókiennictwo.

dr hab. inż. Krzysztof Siczek w roku 1992 ukończył studia na Wydziale Mechanicznym Politechniki Łódzkiej. W 2003 roku uzyskał stopień doktora, a w 2014 doktora habilitowanego na Politechnice Poznańskiej. W 2017 uzyskał doktorat na Wydziale Lekarskim Uniwersytetu Medycznego w Łodzi. Jest zatrudniony na stanowisku adiunkta w Politechnice Łódzkiej w Katedrze Pojazdów i Podstaw Budowy Maszyn. Dziedzina naukowa: Inżynieria Mechaniczna. Zajmuje się zagadnieniami eksploatacji w tym tribologii i wibroakustyki maszyn i urządzeń oraz urządzeń do wytwarzania i gromadzenia energii.

prof. dr hab. inż. Katarzyna Śliżewska – jest pracownikiem naukowo-dydaktycznym na Wydziale Biotechnologii i Nauk o Żywności Politechniki Łódzkiej, zatrudniona na stanowisku profesora. Posiada tytuł profesora w dyscyplinie technologii żywności i żywienia. Zainteresowania naukowe: żywność i pasze o właściwościach prozdrowotnych, ze szczególnym uwzględnieniem probiotyków, prebiotyków oraz mikrobioty jelitowej i chorób dietozależnych. Prowadzi również badania dotyczące detoksykacji substancji szkodliwych. Swoje osiągnięcia naukowe prezentowała na licznych konferencjach krajowych i międzynarodowych. Jest autorką kilkudziesięciu publikacji naukowych z zakresu technologii żywności, żywienia oraz nauk o zdrowiu, a także współautorką patentów. Prowadziła i brała udział w wielu projektach naukowych, często współpracując z otoczeniem społeczno-gospodarczym.

ORCID 0000-0002-3161-1707

mgr. inż. Radosław Świątecki w roku 1996 ukończył studia na Wydziale Inżynierii Procesowej i Ochrony Środowiska Politechnice Łódzkiej. Od tego czasu pracował w licznych zakładach produkcyjnych i firmach na stanowiskach technologicznych. Obecnie jest technologiem w Spółdzielni Inwalidów Zgoda i zajmuje się produkcją odzieży ochronnej.

mgr Malwina Wachulak – absolwentka Uniwersytetu Łódzkiego, gdzie w 2015 roku ukończyła studia magisterskie na kierunku biologia, specjalność: stosowana i molekularna. Jest kierownikiem działu badań i rozwoju w firmie GoudenKorrel S.A., producenta nawozów wieloskładnikowych. Specjalizuje się w opracowywaniu innowacyjnych technologii wspierających efektywność oraz zrównoważony rozwój w rolnictwie, łącząc wiedzę z zakresu biologii molekularnej z jej praktycznym zastosowaniem w przemyśle.

dr inż. Marek Woźniak ukończył studia w roku 2005 na Wydziale Mechanicznym Politechniki Łódzkiej. W 2010 r. uzyskał stopień doktora na Politechnice Łódzkiej. Jest zatrudniony na stanowisku adiunkta w Politechnice Łódzkiej w Katedrze Pojazdów i Podstaw Budowy Maszyn. Dziedzina naukowa: Inżynieria Mechaniczna. Zajmuje się zagadnieniami budowy i eksploatacji pojazdów, maszyn i urządzeń.

mgr Katarzyna Zacharska - jest absolwentką Wydziału Biologii i Ochrony Środowiska Uniwersytetu Łódzkiego. Obecnie pracuje na stanowisku Starszego Specjalisty w Łukasiewicz – Łódzkim Instytucie Technologicznym.